Turkish Journal of Mathematics

Manuscript 3567

Numerical solutions of SIRD model of Covid-19 by utilizing Pell-Lucascollocation method

GAMZE YILDIRIM

ŞUAYİP YÜZBAŞI

Turkish Journal of Mathematics

http://journals.tubitak.gov.tr/math/

Research Article

Turk J Math
(2024) 48: 1156 – 1182
© TÜBİTAK
doi:10.55730/1300-0098.3567

Numerical solutions of SIRD model of Covid-19 by utilizing Pell-Lucas collocation method

Gamze YILDIRIM[1,2], **Şuayip YÜZBAŞI**[3,*]
[1]Department of Mathematics, Faculty of Science, Akdeniz University, Antalya, Turkiye
[2]Department of Mathematics, Faculty of Basic Science, Gebze Technical University, Kocaeli, Turkiye
[3]Department of Mathematics, Faculty of Science, Bartın University, Bartın, Turkiye

Received: 03.05.2024 • **Accepted/Published Online:** 25.09.2024 • **Final Version:** 14.11.2024

Abstract: This article presents an SIRD model based on the evolution of Coronavirus Disease 2019 (COVID-19) caused by SARS-CoV-2 from the coronavirus family. Firstly, we constitute Pell-Lucas collocation method (PLCM) for this model. According to method, the matrix forms of the Pell-Lucas polynomials (PLPs) are constituted. By utilizing this matrix forms, solution forms and all terms in this model are expressed in matrix form. Thus, PLCM transforms our model into a system of the matrix equations. By solving this system, the approximate solutions are obtained. In addition, the error analysis is also presented. In the examples of this study, we analyzed the Türkiye's situation using initial datas and the parameters for Türkiye. For this, we make applications for two different scenarios. In these two scenarios, the parameters, the initial conditions and the selected range are different. By considering the initial data and the parameters for other countries, this method can be applied to them, too. Application results are tabulated and visualized. Moreover, by comparing our results with Runge-Kutta method (RKM), the effectiveness of method is demonstrated. This study allows the identification of trends in the pandemic.

Key words: Collocation method, Covid-19, mathematical modeling, nonlinear differential equations, Pell-Lucas polynomials, SIRD model

1. Introduction

An epidemic of a disease of unknown reason first was emerged in Wuhan, China's Hubei province, in 2019 and spread significantly to other countries. After a short time, this infectious agent was defined as a new coronavirus (nCoV). This virus was named severe acute respiratory syndrome coronavirus 2 (SARS-CoV-2). The World Health Organization (WHO) denominated the infectious disease as coronavirus disease 2019 (COVID-19). WHO announced this situation as a pandemic in March 11, 2020. In this process, some measures were taken around the world. Countries mutually stopped flights and closed border gates. A curfew was imposed, quarantine decisions were made for infected people, education was suspended and distance education was started. Places such as cinemas, concert halls, wedding halls, cafes and massage parlors were temporarily closed. While these negativities were continued, scientists carried out vaccine studies, and after a while, the public was vaccinated to ensure immunity. As the vaccination rate increased, the normalization process began. Although the normalization process has started today, cases and deaths continue. Looking at worldometer data*, as of

*Correspondence: suayipyuzbasi@gmail.com;suayipyuzbasi@bartin.edu.tr

2010 *AMS Mathematics Subject Classification:* 34A34, 42C05, 65L60, 65L70, 92D30, 93A30
*Worldometer, Available from: https://www.worldometers.info/coronavirus/

April 13, 2024, there are a total of 704,753,890 cases, 7,010,681 deaths, and 675,619,811 recoveries, worldwide. Therefore, all studies on this pandemic are important for science and humanity. The mathematicians also started to study this pandemic.

Since the past, the solutions of many mathematical models such as single species models [25, 50, 51, 55, 68, 72, 79], Lotka-Volterra population model [10, 11, 33, 38, 51, 53, 54, 67, 68, 72, 79], Hantavirus infection model [1, 2, 23, 71, 76], HIV (Human Immunodeficiency Virus) infection models [17, 22, 27, 32, 40–42, 46, 58, 61, 64, 69, 70, 73–75], SIR (Susceptible-Infected-Removed) epidemic model [5, 24, 26, 36, 56, 57] and SIRD (Susceptible-Infected-Recovered-Dead) epidemic model [47, 62, 65, 66] have been studied to predict the evolution of infectious diseases by some researchers. Recently, many numerical methods such as the finite element method [6], the multidomain spectral relaxation method [3], the generalized Runge–Kutta method of the fourth order [30] and the spectral collocation approach [31, 35] have been studied to predict the evolution of Covid-19. Since 2020, some researchers have modified SIRD model for Covid-19 data, thus they have predicted the evolution of COVID-19 [14, 15, 19–21, 37, 43, 49]. In 2020, a transmission model with susceptible, infected, recovered and dead classes (SIRD) was developed to understand the spread of COVID-19 in Italy. Official data of the pandemic was used to determine the parameters of this model. According to the results, it can be said that the recovery rate tends to increase over time and the death rate tends to decrease [12]. In 2021, an approach that performs a function estimation used to analyze data on the Covid-19 epidemic in Italy and Brazil. The SIRD model was solved using the Levenberg-Marquardt method. It is concluded that there is a good agreement between the data and the calculated values [13]. In 2021, an SIRD model was used to analyze the evolution of the COVID-19 pandemic caused by SARS-CoV-2 in Spain. MATLAB Ode Solver is used to solve the system. It is concluded that the epidemic is expected to decrease in the following days if adequate isolation measures are maintained. It is stated that the numbers of the recoveries and deaths do not yet show a clear trend and no comment can be made on this issue [39].

On the other hand, some researchers have investigated for Türkiye and estimated the progress of COVID-19 using some methods [4, 7–9, 16, 45, 48, 63]. In 2021, the SIRD epidemic model used to study the evolution of COVID-19 in some countries. Numerical simulations performed for France, Italy, Germany, Russia, Hungary, Canada, Iran, Ukraine, Japan, Türkiye, Pakistan, Lithuania, Uganda and the USA. The results estimated by the finite difference method. According to the data, it is estimated that if the rate of spread decreases, the number of the confirmed cases and the maximum number of the infected cases decrease greatly [52]. Also, Yüzbaşı and Yıldırım applied Pell-Lucas collocation method (PLCM) for solving SIR model with Türkiye's Covid-19 info [78]. The difference of the presented research from the study [78] is that the removed class is applied as two separate classes (the recovered class and the dead class). In study [78], the removed class gave us total information about the recovered class and dead class. Accordingly, there is no information available to compare the recovered class with the dead class. For this reason, it is important to consider this class sThe matrix formeparately as the recovered class and the dead class. Thanks to this study, it will be possible to determine how many people died and recovered from the total population after days such as 60 days and 300 days, which we considered in the applications section.

The advantage of our method is that the results can be quickly obtained by using the code created in MATLAB. Other advantage of our method is that other advantage of our method is that effective outcomes can be obtained from our method even if the selected N value is very small. Another advantage of our method is that the structure of the collocation method is simple and the computational cost is low. It also provides a very easy and simple procedure for solving various problems involving differential equations that model real-world phenomena. In the literature, there are many numerical methods via Pell-Lucas polynomials (PLPs) for various types of differential equations [18, 59, 60, 77, 79–81]. According to these studies, it is concluded that successful outputs are discovered via PLPs. However, in the literature, there is no study based on a method using PLPs for solving SIRD model. For this reason, in this paper, by adapting this model for Türkiye's Covid-19 data, PLCM is developed. In this article, SIRD epidemic model are given by [13, 15, 19]

$$\begin{aligned}
&\frac{d\mathcal{S}(t)}{dt} = -\frac{\beta}{\mathcal{P}}\mathcal{S}(t)\mathcal{I}(t)\\
&\frac{d\mathcal{I}(t)}{dt} = \frac{\beta}{\mathcal{P}}\mathcal{S}(t)\mathcal{I}(t) - \gamma\mathcal{I}(t) - \delta\mathcal{I}(t)\\
&\frac{d\mathcal{R}(t)}{dt} = \gamma\mathcal{I}(t)\\
&\frac{d\mathcal{D}(t)}{dt} = \delta\mathcal{I}(t)\\
&\mathcal{S}(0) = S_0, \quad \mathcal{I}(0) = I_0, \quad \mathcal{R}(0) = R_0, \quad \mathcal{D}(0) = D_0.
\end{aligned} \tag{1.1}$$

Here, $\mathcal{S}(t)$, $\mathcal{I}(t)$, $\mathcal{R}(t)$ and $\mathcal{D}(t)$ represent, respectively, the susceptible, infected, recovered and dead population defined on the interval $0 \le t \le b$. β, γ, δ are transmission rate, recovery rate and death rate, respectively. P is total population and $\mathcal{P} = \mathcal{S}(t) + \mathcal{I}(t) + \mathcal{R}(t) + \mathcal{D}(t)$. Figure 1 shows the flow between four classes of the model with arrows.

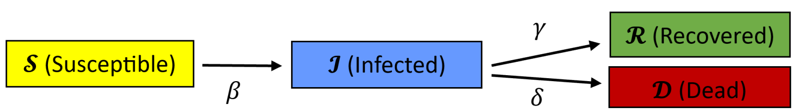

Figure 1. Diagram of modeling of (1.1).

For SIRD epidemic model to be applicable, the model has some prerequisites. These prerequisites are described below:

- The equations that arise when time is divided into a series of discrete intervals are considered and the infections are assumed to occur only at the moment of transition from one interval to another.
- Natural birth and natural death are assumed to be neglected.
- It is assumed that all individuals in the population are equally likely to be infected.
- Age, gender, race and social status do not affect the probability of an individual being infected.
- The parameters representing the transmission rate and recovery rate for each individual are assumed to be at a constant value throughout the course of the disease.

The aim of this paper is to obtain approximate solutions of (1.1) as

$$\begin{aligned}
\mathcal{S}_N(t) &= \textstyle\sum_{n=0}^{N} a_n Q_n(t),\\
\mathcal{I}_N(t) &= \textstyle\sum_{n=0}^{N} b_n Q_n(t),\\
\mathcal{R}_N(t) &= \textstyle\sum_{n=0}^{N} c_n Q_n(t),\\
\mathcal{D}_N(t) &= \textstyle\sum_{n=0}^{N} d_n Q_n(t).
\end{aligned} \tag{1.2}$$

Here, $N > 0$ and a_n, b_n, c_n, d_n represent the unknown coefficients. $Q_n(t)$ represents PLPs and it is described as follows [28, 29]:

$$Q_j(t) = \sum_{i=0}^{[\![j/2]\!]} 2^{j-2i} \frac{j}{j-i} \binom{j-i}{i} t^{j-2i}$$

where $[\![j/2]\!]$ is the integer value of $j/2$. Please see [28, 29], for features about PLPs.

This article is organized as follows: In Section 2, the required matrix relations for our method are presented. In Section 3, the Pell-Lucas collocation method for SIRD model is presented. In Section 4, the error analysis is given. In Section 5, the parameters and initial conditions in the SIR model are determined according to Türkiye's Covid-19 data. Thus, PLCM is applied to this model. Simulation results are presented and evaluated in tables and graphs. In Section 6, a brief conclusion of the article is presented.

2. Basic matrix relations

The aim of this part is to express the Pell-Lucas polynomial solutions (PLPS) and each term in the SIRD model (1.1) in matrix form.

Lemma 2.1 *The matrix form [78, 79]. of PLPs is*

$$\mathbf{Q}_N(t) = \mathbf{T}_N(t)\mathbf{M}_N. \tag{2.1}$$

Here, $\mathbf{Q}_N(t) = \begin{bmatrix} Q_0(t) & Q_1(t) & Q_2(t) & \cdots & Q_N(t) \end{bmatrix}$ *and* $\mathbf{T}_N(t) = \begin{bmatrix} 1 & t & t^2 & \cdots & t^N \end{bmatrix}$. *If N is odd*

$$\mathbf{M}_N^T = \begin{bmatrix} 2 & 0 & 0 & \cdots & 0 \\ 0 & 2^1 \frac{1}{1}\binom{1}{0} & 0 & \cdots & 0 \\ 2^0 \frac{2}{1}\binom{1}{1} & 0 & 2^2 \frac{2}{2}\binom{2}{0} & \cdots & 0 \\ \vdots & \vdots & \vdots & \ddots & \vdots \\ 0 & 2^1 \frac{N}{\frac{N+1}{2}}\binom{\frac{N+1}{2}}{\frac{N-1}{2}} & 0 & \cdots & 2^N \frac{N}{N}\binom{N}{0} \end{bmatrix}$$

and if N is even

$$\mathbf{M}_N^T = \begin{bmatrix} 2 & 0 & 0 & \cdots & 0 \\ 0 & 2^1 \frac{1}{1}\binom{1}{0} & 0 & \cdots & 0 \\ 2^0 \frac{2}{1}\binom{1}{1} & 0 & 2^2 \frac{2}{2}\binom{2}{0} & \cdots & 0 \\ \vdots & \vdots & \vdots & \ddots & \vdots \\ 2^0 \frac{N}{\frac{N}{2}}\binom{\frac{N}{2}}{\frac{N}{2}} & 0 & 2^2 \frac{N}{\frac{N+2}{2}}\binom{\frac{N+2}{2}}{\frac{N-2}{2}} & \cdots & 2^N \frac{N}{N}\binom{N}{0} \end{bmatrix}.$$

Proof By multiplying the vector $\mathbf{T}_N(t)$ by the matrix $\mathbf{M}_N$ from the right side, the vector $\mathbf{T}_N(t)\mathbf{M}_N$ is obtained, which is $\mathbf{Q}_N(t)$. □

Lemma 2.2 *PLPS (1.2) of SIRD model (1.1) are written in matrix forms:*

$$\begin{aligned} \mathcal{S}_N(t) &= \mathbf{T}_N(t)\mathbf{M}_N\mathbf{A}_N \\ \mathcal{I}_N(t) &= \mathbf{T}_N(t)\mathbf{M}_N\mathbf{B}_N \\ \mathcal{R}_N(t) &= \mathbf{T}_N(t)\mathbf{M}_N\mathbf{C}_N \\ \mathcal{D}_N(t) &= \mathbf{T}_N(t)\mathbf{M}_N\mathbf{D}_N. \end{aligned} \tag{2.2}$$

Here,

$$\mathbf{A}_N = \begin{bmatrix} a_0 & a_1 & \cdots & a_N \end{bmatrix}^T, \quad \mathbf{B}_N = \begin{bmatrix} b_0 & b_1 & \cdots & b_N \end{bmatrix}^T, \quad \mathbf{C}_N = \begin{bmatrix} c_0 & c_1 & \cdots & c_N \end{bmatrix}^T, \quad \mathbf{D}_N = \begin{bmatrix} d_0 & d_1 & \cdots & d_N \end{bmatrix}^T.$$

Also, other matrices are expressed in Lemma 2.1.

Proof By multiplying $\mathbf{T}_N(t)\mathbf{M}_N$, respectively, by $\mathbf{A}_N$, $\mathbf{B}_N$, $\mathbf{C}_N$, $\mathbf{D}_N$ from the right, we get (2.2), which completes the proof. □

Lemma 2.3 *The derivatives of PLPS (2.2) are expressed as follows:*

$$\begin{aligned} \mathcal{S}_N'(t) &= \mathbf{T}_N(t)\mathbf{F}_N\mathbf{M}_N\mathbf{A}_N \\ \mathcal{I}_N'(t) &= \mathbf{T}_N(t)\mathbf{F}_N\mathbf{M}_N\mathbf{B}_N \\ \mathcal{R}_N'(t) &= \mathbf{T}_N(t)\mathbf{F}_N\mathbf{M}_N\mathbf{C}_N \\ \mathcal{D}_N'(t) &= \mathbf{T}_N(t)\mathbf{F}_N\mathbf{M}_N\mathbf{D}_N. \end{aligned} \tag{2.3}$$

Here,

$$\mathbf{F}_N = \begin{bmatrix} 0 & 1 & 0 & \cdots & 0 \\ 0 & 0 & 2 & \cdots & 0 \\ \vdots & \vdots & \vdots & \ddots & \vdots \\ 0 & 0 & 0 & \cdots & N \\ 0 & 0 & 0 & \cdots & 0 \end{bmatrix}.$$

And other matrices are expressed in Lemma 2.2.

Proof The first derivatives of PLPS (2.2) are in forms:

$$\begin{aligned} \mathcal{S}_N'(t) &= \mathbf{T}_N'(t)\mathbf{M}_N\mathbf{A}_N \\ \mathcal{I}_N'(t) &= \mathbf{T}_N'(t)\mathbf{M}_N\mathbf{B}_N \\ \mathcal{R}_N'(t) &= \mathbf{T}_N'(t)\mathbf{M}_N\mathbf{C}_N \\ \mathcal{D}_N'(t) &= \mathbf{T}_N'(t)\mathbf{M}_N\mathbf{D}_N. \end{aligned} \tag{2.4}$$

On the other hand, by taking the first derivative of $\mathbf{T}_N(t)$, it is obtained

$$\mathbf{T}_N'(t) = \mathbf{T}_N(t)\mathbf{F}_N. \tag{2.5}$$

Thus, by substituting the relation (2.5) in (2.4), the derivatives of PLPS (2.2) are expressed as in (2.3).
□

Lemma 2.4 *The nonlinear expression $\mathcal{S}(t)\mathcal{I}(t)$ in SIRD model (1.1) can be written as*

$$\mathcal{S}_N(t)\mathcal{I}_N(t) = \left(\mathbf{T}_N(t)\mathbf{M}_N\mathbf{A}_N\right)\left(\mathbf{T}_N(t)\mathbf{M}_N\mathbf{B}_N\right). \tag{2.6}$$

The matrices $\mathbf{T}_N(t)$, $\mathbf{M}_N$, $\mathbf{A}_N$ and $\mathbf{B}_N$ in (2.6) are expressed in Lemma 2.2.

Proof Utilizing Lemma 2.2, we can write $\mathcal{S}_N(t) = \mathbf{T}_N(t)\mathbf{M}_N\mathbf{A}_N$ and $\mathcal{I}_N(t) = \mathbf{T}_N(t)\mathbf{M}_N\mathbf{B}_N$. By multiplying the matrix product $\mathcal{S}_N(t)$ by the matrix product $\mathcal{I}_N(t)$ from the right side, we get (2.6). □

Lemma 2.5 *The initial conditions in the SIRD model (1.1) are expressed as follows:*

$$\begin{aligned} \mathbf{U}_N\mathbf{A}_N &= \mathcal{S}_0, \\ \mathbf{U}_N\mathbf{B}_N &= \mathcal{I}_0, \\ \mathbf{U}_N\mathbf{C}_N &= \mathcal{R}_0, \\ \mathbf{U}_N\mathbf{D}_N &= \mathcal{D}_0. \end{aligned} \tag{2.7}$$

Here, $\mathbf{U}_N = \mathbf{T}_N(0)\mathbf{M}_N$. *The matrices* $\mathbf{T}_N(t)$, $\mathbf{M}_N$, $\mathbf{A}_N$, $\mathbf{B}_N$, $\mathbf{C}_N$ *and* $\mathbf{D}_N$ *in (2.7) are expressed in Lemma 2.2.*

Proof If $t \to 0$ in (2.2), then we get

$$\begin{aligned} \mathcal{S}_N(0) &= \mathbf{T}_N(0)\mathbf{M}_N\mathbf{A}_N \\ \mathcal{I}_N(0) &= \mathbf{T}_N(0)\mathbf{M}_N\mathbf{B}_N \\ \mathcal{R}_N(0) &= \mathbf{T}_N(0)\mathbf{M}_N\mathbf{C}_N \\ \mathcal{D}_N(0) &= \mathbf{T}_N(0)\mathbf{M}_N\mathbf{D}_N. \end{aligned} \tag{2.8}$$

Finally, the matrix multiplication $\mathbf{T}_N(0)\mathbf{M}_N$ is denoted as $\mathbf{U}_N$ and so we gain (2.7). □

Theorem 2.6 *Suppose that the solutions of the SIRD model (1.1) are represented as in (1.2). Then, we have*

$$\begin{aligned} \mathbf{T}_N(t)\mathbf{F}_N\mathbf{M}_N\mathbf{A}_N &= -\tfrac{\beta}{\mathcal{P}}\left(\mathbf{T}_N(t)\mathbf{M}_N\mathbf{A}_N\right)\left(\mathbf{T}_N(t)\mathbf{M}_N\mathbf{B}_N\right) \\ \mathbf{T}_N(t)\mathbf{F}_N\mathbf{M}_N\mathbf{B}_N &= \tfrac{\beta}{\mathcal{P}}\left(\mathbf{T}_N(t)\mathbf{M}_N\mathbf{A}_N\right)\left(\mathbf{T}_N(t)\mathbf{M}_N\mathbf{B}_N\right) - \gamma\mathbf{T}_N(t)\mathbf{M}_N\mathbf{B}_N - \delta\mathbf{T}_N(t)\mathbf{M}_N\mathbf{B}_N \\ \mathbf{T}_N(t)\mathbf{F}_N\mathbf{M}_N\mathbf{C}_N &= \gamma\left(\mathbf{T}_N(t)\mathbf{M}_N\mathbf{B}_N\right) \\ \mathbf{T}_N(t)\mathbf{F}_N\mathbf{M}_N\mathbf{D}_N &= \delta\left(\mathbf{T}_N(t)\mathbf{M}_N\mathbf{B}_N\right). \end{aligned} \tag{2.9}$$

All matrices are expressed in Lemmas 2.2 and 2.3.

Proof By using Lemmas 2.2-2.4 for the solutions forms, derivative terms and the nonlinear terms in (1.1), the proof is completed. □

3. PLCM for the SIRD model

In this section, the method is created with the help of the collocation points and the matrix relations in the previous section.

Definition 3.1 *The collocation points for the range of* $[0, b]$ *are described by*

$$t_i = \frac{b}{N}i, \quad i = 0, 1, ..., N. \tag{3.1}$$

Theorem 3.2 *Assume that the approximate solutions of the SIRD model (1.1) are investigated in the matrix forms (2.2). Then, model (1.1) becomes*

$$\begin{aligned}
\mathbf{W}_0\mathbf{A}_N + \mathbf{G}_{1,0}\mathbf{B}_N &= 0\\
\mathbf{W}_0\mathbf{B}_N + \mathbf{G}_{2,0}\mathbf{B}_N &= 0\\
\mathbf{W}_0\mathbf{C}_N + \mathbf{G}_{3,0}\mathbf{B}_N &= 0\\
\mathbf{W}_0\mathbf{D}_N + \mathbf{G}_{4,0}\mathbf{B}_N &= 0\\
\mathbf{W}_1\mathbf{A}_N + \mathbf{G}_{1,1}\mathbf{B}_N &= 0\\
\mathbf{W}_1\mathbf{B}_N + \mathbf{G}_{2,1}\mathbf{B}_N &= 0\\
\mathbf{W}_1\mathbf{C}_N + \mathbf{G}_{3,1}\mathbf{B}_N &= 0\\
\mathbf{W}_1\mathbf{D}_N + \mathbf{G}_{4,1}\mathbf{B}_N &= 0\\
&\vdots\\
\mathbf{W}_N\mathbf{A}_N + \mathbf{G}_{1,N}\mathbf{B}_N &= 0\\
\mathbf{W}_N\mathbf{B}_N + \mathbf{G}_{2,N}\mathbf{B}_N &= 0\\
\mathbf{W}_N\mathbf{C}_N + \mathbf{G}_{3,N}\mathbf{B}_N &= 0\\
\mathbf{W}_N\mathbf{D}_N + \mathbf{G}_{4,N}\mathbf{B}_N &= 0.
\end{aligned} \tag{3.2}$$

Here,

$$\begin{aligned}
&\mathbf{W}_i = \mathbf{T}_N(t_i)\mathbf{F}_N\mathbf{M}_N,\\
&\mathbf{G}_{1,i} = \tfrac{\beta}{\mathcal{P}}\left(\mathbf{T}_N(t_i)\mathbf{M}_N\mathbf{A}_N\right)\mathbf{T}_N(t_i)\mathbf{M}_N,\\
&\mathbf{G}_{2,i} = -\tfrac{\beta}{\mathcal{P}}\left(\mathbf{T}_N(t_i)\mathbf{M}_N\mathbf{A}_N\right)\mathbf{T}_N(t_i)\mathbf{M}_N + \gamma\mathbf{T}_N(t_i)\mathbf{M}_N + \delta\mathbf{T}_N(t_i)\mathbf{M}_N,\\
&\mathbf{G}_{3,i} = -\gamma\mathbf{T}_N(t_i)\mathbf{M}_N,\\
&\mathbf{G}_{4,i} = -\delta\mathbf{T}_N(t_i)\mathbf{M}_N.
\end{aligned}$$

The matrices here are also given in Lemmas 2.1 - 2.3.

Proof By substituting (3.1) into (2.9), then we have

$$\begin{aligned}
&\mathbf{T}_N(t_0)\mathbf{F}_N\mathbf{M}_N\mathbf{A}_N = -\tfrac{\beta}{\mathcal{P}}\left(\mathbf{T}_N(t_0)\mathbf{M}_N\mathbf{A}_N\right)\left(\mathbf{T}_N(t_0)\mathbf{M}_N\mathbf{B}_N\right)\\
&\mathbf{T}_N(t_0)\mathbf{F}_N\mathbf{M}_N\mathbf{B}_N = \tfrac{\beta}{\mathcal{P}}\left(\mathbf{T}_N(t_0)\mathbf{M}_N\mathbf{A}_N\right)\left(\mathbf{T}_N(t_0)\mathbf{M}_N\mathbf{B}_N\right) - \gamma\mathbf{T}_N(t_0)\mathbf{M}_N\mathbf{B}_N - \delta\mathbf{T}_N(t_0)\mathbf{M}_N\mathbf{B}_N\\
&\mathbf{T}_N(t_0)\mathbf{F}_N\mathbf{M}_N\mathbf{C}_N = \gamma\left(\mathbf{T}_N(t_0)\mathbf{M}_N\mathbf{B}_N\right)\\
&\mathbf{T}_N(t_0)\mathbf{F}_N\mathbf{M}_N\mathbf{D}_N = \delta\left(\mathbf{T}_N(t_0)\mathbf{M}_N\mathbf{B}_N\right)\\
&\mathbf{T}_N(t_1)\mathbf{F}_N\mathbf{M}_N\mathbf{A}_N = -\tfrac{\beta}{\mathcal{P}}\left(\mathbf{T}_N(t_1)\mathbf{M}_N\mathbf{A}_N\right)\left(\mathbf{T}_N(t_1)\mathbf{M}_N\mathbf{B}_N\right)\\
&\mathbf{T}_N(t_1)\mathbf{F}_N\mathbf{M}_N\mathbf{B}_N = \tfrac{\beta}{\mathcal{P}}\left(\mathbf{T}_N(t_1)\mathbf{M}_N\mathbf{A}_N\right)\left(\mathbf{T}_N(t_1)\mathbf{M}_N\mathbf{B}_N\right) - \gamma\mathbf{T}_N(t_1)\mathbf{M}_N\mathbf{B}_N - \delta\mathbf{T}_N(t_1)\mathbf{M}_N\mathbf{B}_N\\
&\mathbf{T}_N(t_1)\mathbf{F}_N\mathbf{M}_N\mathbf{C}_N = \gamma\left(\mathbf{T}_N(t_1)\mathbf{M}_N\mathbf{B}_N\right)\\
&\mathbf{T}_N(t_1)\mathbf{F}_N\mathbf{M}_N\mathbf{D}_N = \delta\left(\mathbf{T}_N(t_1)\mathbf{M}_N\mathbf{B}_N\right)\\
&\qquad\qquad\qquad\vdots\\
&\mathbf{T}_N(t_N)\mathbf{F}_N\mathbf{M}_N\mathbf{A}_N = -\tfrac{\beta}{\mathcal{P}}\left(\mathbf{T}_N(t_N)\mathbf{M}_N\mathbf{A}_N\right)\left(\mathbf{T}_N(t_N)\mathbf{M}_N\mathbf{B}_N\right)\\
&\mathbf{T}_N(t_N)\mathbf{F}_N\mathbf{M}_N\mathbf{B}_N = \tfrac{\beta}{\mathcal{P}}\left(\mathbf{T}_N(t_N)\mathbf{M}_N\mathbf{A}_N\right)\left(\mathbf{T}_N(t_N)\mathbf{M}_N\mathbf{B}_N\right) - \gamma\mathbf{T}_N(t_N)\mathbf{M}_N\mathbf{B}_N - \delta\mathbf{T}_N(t_N)\mathbf{M}_N\mathbf{B}_N\\
&\mathbf{T}_N(t_N)\mathbf{F}_N\mathbf{M}_N\mathbf{C}_N = \gamma\left(\mathbf{T}_N(t_N)\mathbf{M}_N\mathbf{B}_N\right)\\
&\mathbf{T}_N(t_N)\mathbf{F}_N\mathbf{M}_N\mathbf{D}_N = \delta\left(\mathbf{T}_N(t_N)\mathbf{M}_N\mathbf{B}_N\right)
\end{aligned} \tag{3.3}$$

or

$$\begin{gathered}
\mathbf{W}_0\mathbf{A}_N + \mathbf{G}_{1,0}\mathbf{B}_N = 0 \\
\mathbf{W}_0\mathbf{B}_N + \mathbf{G}_{2,0}\mathbf{B}_N = 0 \\
\mathbf{W}_0\mathbf{C}_N + \mathbf{G}_{3,0}\mathbf{B}_N = 0 \\
\mathbf{W}_0\mathbf{D}_N + \mathbf{G}_{4,0}\mathbf{B}_N = 0 \\
\mathbf{W}_1\mathbf{A}_N + \mathbf{G}_{1,1}\mathbf{B}_N = 0 \\
\mathbf{W}_1\mathbf{B}_N + \mathbf{G}_{2,1}\mathbf{B}_N = 0 \\
\mathbf{W}_1\mathbf{C}_N + \mathbf{G}_{3,1}\mathbf{B}_N = 0 \\
\mathbf{W}_1\mathbf{D}_N + \mathbf{G}_{4,1}\mathbf{B}_N = 0 \\
\vdots \\
\mathbf{W}_N\mathbf{A}_N + \mathbf{G}_{1,N}\mathbf{B}_N = 0 \\
\mathbf{W}_N\mathbf{B}_N + \mathbf{G}_{2,N}\mathbf{B}_N = 0 \\
\mathbf{W}_N\mathbf{C}_N + \mathbf{G}_{3,N}\mathbf{B}_N = 0 \\
\mathbf{W}_N\mathbf{D}_N + \mathbf{G}_{4,N}\mathbf{B}_N = 0.
\end{gathered}$$

Finally, if the following equations are also used

$$\begin{aligned}
&\mathbf{W}_i = \mathbf{T}_N(t_i)\mathbf{F}_N\mathbf{M}_N, \\
&\mathbf{G}_{1,i} = \tfrac{\beta}{\mathcal{P}}\left(\mathbf{T}_N(t_i)\mathbf{M}_N\mathbf{A}_N\right)\mathbf{T}_N(t_i)\mathbf{M}_N, \\
&\mathbf{G}_{2,i} = -\tfrac{\beta}{\mathcal{P}}\left(\mathbf{T}_N(t_i)\mathbf{M}_N\mathbf{A}_N\right)\mathbf{T}_N(t_i)\mathbf{M}_N + \gamma\mathbf{T}_N(t_i)\mathbf{M}_N + \delta\mathbf{T}_N(t_i)\mathbf{M}_N, \\
&\mathbf{G}_{3,i} = -\gamma\mathbf{T}_N(t_i)\mathbf{M}_N, \\
&\mathbf{G}_{4,i} = -\delta\mathbf{T}_N(t_i)\mathbf{M}_N,
\end{aligned}$$

the proof is completed. □

Theorem 3.3 *Assume that the solutions of SIRD model (1.1) are investigated in the matrix forms (2.2). In that case, the following system is obtained:*

$$\begin{gathered}
\mathbf{W}_0\mathbf{A}_N + \mathbf{G}_{1,0}\mathbf{B}_N = 0 \\
\mathbf{W}_0\mathbf{B}_N + \mathbf{G}_{2,0}\mathbf{B}_N = 0 \\
\mathbf{W}_0\mathbf{C}_N + \mathbf{G}_{3,0}\mathbf{B}_N = 0 \\
\mathbf{W}_0\mathbf{D}_N + \mathbf{G}_{4,0}\mathbf{B}_N = 0 \\
\mathbf{W}_1\mathbf{A}_N + \mathbf{G}_{1,1}\mathbf{B}_N = 0 \\
\mathbf{W}_1\mathbf{B}_N + \mathbf{G}_{2,1}\mathbf{B}_N = 0 \\
\mathbf{W}_1\mathbf{C}_N + \mathbf{G}_{3,1}\mathbf{B}_N = 0 \\
\mathbf{W}_1\mathbf{D}_N + \mathbf{G}_{4,1}\mathbf{B}_N = 0 \\
\vdots \\
\mathbf{W}_N\mathbf{A}_N + \mathbf{G}_{1,N}\mathbf{B}_N = 0 \\
\mathbf{W}_N\mathbf{B}_N + \mathbf{G}_{2,N}\mathbf{B}_N = 0 \\
\mathbf{W}_N\mathbf{C}_N + \mathbf{G}_{3,N}\mathbf{B}_N = 0 \\
\mathbf{W}_N\mathbf{D}_N + \mathbf{G}_{4,N}\mathbf{B}_N = 0 \\
\mathbf{U}_N\mathbf{A}_N = \mathcal{S}_0 \\
\mathbf{U}_N\mathbf{B}_N = \mathcal{I}_0 \\
\mathbf{U}_N\mathbf{C}_N = \mathcal{R}_0 \\
\mathbf{U}_N\mathbf{D}_N = \mathcal{D}_0.
\end{gathered} \tag{3.4}$$

The matrices in here are also expressed in Theorem 3.2 and Lemma 2.5.

Proof By writing the matrix systems (2.7) and (3.2) as one system, a new matrix system ($4(N+2)\times 1$-dimensional) is obtained as:

$$\begin{array}{c} \mathbf{W}_0\mathbf{A}_N + \mathbf{G}_{1,0}\mathbf{B}_N = 0 \\ \mathbf{W}_0\mathbf{B}_N + \mathbf{G}_{2,0}\mathbf{B}_N = 0 \\ \mathbf{W}_0\mathbf{C}_N + \mathbf{G}_{3,0}\mathbf{B}_N = 0 \\ \mathbf{W}_0\mathbf{D}_N + \mathbf{G}_{4,0}\mathbf{B}_N = 0 \\ \mathbf{W}_1\mathbf{A}_N + \mathbf{G}_{1,1}\mathbf{B}_N = 0 \\ \mathbf{W}_1\mathbf{B}_N + \mathbf{G}_{2,1}\mathbf{B}_N = 0 \\ \mathbf{W}_1\mathbf{C}_N + \mathbf{G}_{3,1}\mathbf{B}_N = 0 \\ \mathbf{W}_1\mathbf{D}_N + \mathbf{G}_{4,1}\mathbf{B}_N = 0 \\ \vdots \\ \mathbf{W}_N\mathbf{A}_N + \mathbf{G}_{1,N}\mathbf{B}_N = 0 \\ \mathbf{W}_N\mathbf{B}_N + \mathbf{G}_{2,N}\mathbf{B}_N = 0 \\ \mathbf{W}_N\mathbf{C}_N + \mathbf{G}_{3,N}\mathbf{B}_N = 0 \\ \mathbf{W}_N\mathbf{D}_N + \mathbf{G}_{4,N}\mathbf{B}_N = 0 \\ \mathbf{U}_N\mathbf{A}_N = \mathcal{S}_0 \\ \mathbf{U}_N\mathbf{B}_N = \mathcal{I}_0 \\ \mathbf{U}_N\mathbf{C}_N = \mathcal{R}_0 \\ \mathbf{U}_N\mathbf{D}_N = \mathcal{D}_0. \end{array} \tag{3.5}$$

Here,

$$\begin{aligned} &\mathbf{W}_i = \mathbf{T}_N(t_i)\mathbf{F}_N\mathbf{M}_N, \\ &\mathbf{G}_{1,i} = \tfrac{\beta}{\mathcal{P}}\left(\mathbf{T}_N(t_i)\mathbf{M}_N\mathbf{A}_N\right)\mathbf{T}_N(t_i)\mathbf{M}_N, \\ &\mathbf{G}_{2,i} = -\tfrac{\beta}{\mathcal{P}}\left(\mathbf{T}_N(t_i)\mathbf{M}_N\mathbf{A}_N\right)\mathbf{T}_N(t_i)\mathbf{M}_N + \gamma\mathbf{T}_N(t_i)\mathbf{M}_N + \delta\mathbf{T}_N(t_i)\mathbf{M}_N, \\ &\mathbf{G}_{3,i} = -\gamma\mathbf{T}_N(t_i)\mathbf{M}_N, \\ &\mathbf{G}_{4,i} = -\delta\mathbf{T}_N(t_i)\mathbf{M}_N, \\ &\mathbf{U}_N = \mathbf{T}_N(0)\mathbf{M}_N. \end{aligned}$$

Other matrices are expressed in Theorem 2.6. Thus, the desired results are achieved. □

Corollary 3.4 *The obtained system (3.4) is solved according to the PLCM by using a program written in MATLAB and thus we gain PLPS of (1.1).*

4. Error analysis

In this section, the upper boundary of the errors are determined and the residual error estimation technique is presented. The exact solutions of the SIRD model (1.1) are indicated by $\mathcal{S}(t)$, $\mathcal{I}(t)$, $\mathcal{R}(t)$, $\mathcal{D}(t)$ and the approximate solutions are indicated by $\mathcal{S}_N(t)$, $\mathcal{I}_N(t)$, $\mathcal{R}_N(t)$, $\mathcal{D}_N(t)$. The expansions of Maclaurin series are indicated by $\mathcal{S}_N^M(t)$, $\mathcal{I}_N^M(t)$, $\mathcal{R}_N^M(t)$, $\mathcal{D}_N^M(t)$. Also, the residual functions of the SIRD model (1.1) are represented, respectively, $Re_{i,N}(t)$ $(i=1,2,3,4)$. The error analysis is performed for the SIR model [78]. In this section, we make similarly by utilizing this work.

Theorem 4.1 *(Upper Boundary of Errors) The absolute errors of PLPS are limited by inequalities*

$$\begin{aligned} &\|\mathcal{S}(t)-\mathcal{S}_N(t)\|_\infty \le v_N(\|\widetilde{\mathbf{A}}_N\|_\infty + \|\mathbf{M}_N\|_\infty\|\mathbf{A}_N\|_\infty) + \tfrac{b^{N+1}}{(N+1)!}\|\mathcal{S}^{(N+1)}(c_t)\|_\infty \\ &\|\mathcal{I}(t)-\mathcal{I}_N(t)\|_\infty \le v_N(\|\widetilde{\mathbf{B}}_N\|_\infty + \|\mathbf{M}_N\|_\infty\|\mathbf{B}_N\|_\infty) + \tfrac{b^{N+1}}{(N+1)!}\|\mathcal{I}^{(N+1)}(c_t)\|_\infty \\ &\|\mathcal{R}(t)-\mathcal{R}_N(t)\|_\infty \le v_N(\|\widetilde{\mathbf{C}}_N\|_\infty + \|\mathbf{M}_N\|_\infty\|\mathbf{C}_N\|_\infty) + \tfrac{b^{N+1}}{(N+1)!}\|\mathcal{R}^{(N+1)}(c_t)\|_\infty \\ &\|\mathcal{D}(t)-\mathcal{D}_N(t)\|_\infty \le v_N(\|\widetilde{\mathbf{D}}_N\|_\infty + \|\mathbf{M}_N\|_\infty\|\mathbf{D}_N\|_\infty) + \tfrac{b^{N+1}}{(N+1)!}\|\mathcal{D}^{(N+1)}(c_t)\|_\infty \end{aligned} \tag{4.1}$$

where $\|\mathbf{T}_N(t)\|_\infty \le \max\{b^N,1\} := v_N$, $0 \le t \le b$, $\triangle\mathbf{A}_N = \|\mathbf{A}_{N+1}\|_\infty - \|\mathbf{A}_N\|_\infty$, $\triangle\mathbf{B}_N = \|\mathbf{B}_{N+1}\|_\infty - \|\mathbf{B}_N\|_\infty$, $\triangle\mathbf{C}_N = \|\mathbf{C}_{N+1}\|_\infty - \|\mathbf{C}_N\|_\infty$, $\triangle\mathbf{D}_N = \|\mathbf{D}_{N+1}\|_\infty - \|\mathbf{D}_N\|_\infty$. *In addition,* $\widetilde{\mathbf{A}}_N$ *represents the coefficient matrix of* $\mathcal{S}_N^M(t)$, $\widetilde{\mathbf{B}}_N$ *represents the coefficient matrix of* $\mathcal{I}_N^M(t)$, $\widetilde{\mathbf{C}}_N$ *represents the coefficient matrix of* $\mathcal{R}_N^M(t)$ *and* $\widetilde{\mathbf{D}}_N$ *represents the coefficient matrix of* $\mathcal{D}_N^M(t)$.

Proof As the first step, the Maclaurin expansions are added and then subtracted, respectively, by $S(t)-S_N(t)$, $I(t)-I_N(t)$, $R(t)-R_N(t)$, $D(t)-D_N(t)$. Then, by using the triangle inequality, it is written

$$\begin{aligned}
\|\mathcal{S}(t)-\mathcal{S}_N(t)\|_\infty &= \|\mathcal{S}(t)-\mathcal{S}_N^M(t)+\mathcal{S}_N^M(t)-\mathcal{S}_N(t)\|_\infty \le \|\mathcal{S}(t)-\mathcal{S}_N^M(t)\|_\infty + \|\mathcal{S}_N^M(t)-\mathcal{S}_N(t)\|_\infty\\
\|\mathcal{I}(t)-\mathcal{I}_N(t)\|_\infty &= \|\mathcal{I}(t)-\mathcal{I}_N^M(t)+\mathcal{I}_N^M(t)-\mathcal{I}_N(t)\|_\infty \le \|\mathcal{I}(t)-\mathcal{I}_N^M(t)\|_\infty + \|\mathcal{I}_N^M(t)-\mathcal{I}_N(t)\|_\infty\\
\|\mathcal{R}(t)-\mathcal{R}_N(t)\|_\infty &= \|\mathcal{R}(t)-\mathcal{R}_N^M(t)+\mathcal{R}_N^M(t)-\mathcal{R}_N(t)\|_\infty \le \|\mathcal{R}(t)-\mathcal{R}_N^M(t)\|_\infty + \|\mathcal{R}_N^M(t)-\mathcal{R}_N(t)\|_\infty\\
\|\mathcal{D}(t)-\mathcal{D}_N(t)\|_\infty &= \|\mathcal{D}(t)-\mathcal{D}_N^M(t)+\mathcal{D}_N^M(t)-\mathcal{D}_N(t)\|_\infty \le \|\mathcal{D}(t)-\mathcal{D}_N^M(t)\|_\infty + \|\mathcal{D}_N^M(t)-\mathcal{D}_N(t)\|_\infty.
\end{aligned} \tag{4.2}$$

Now, let us examine the terms $\|\mathcal{S}(t)-\mathcal{S}_N^M(t)\|_\infty$, $\|\mathcal{I}(t)-\mathcal{I}_N^M(t)\|_\infty$, $\|\mathcal{R}(t)-\mathcal{R}_N^M(t)\|_\infty$, $\|\mathcal{D}(t)-\mathcal{D}_N^M(t)\|_\infty$. The remainder terms of the expansions of the Maclaurin series are expressed as follows:

$$\begin{aligned}
&\tfrac{t^{N+1}}{(N+1)!}\mathcal{S}^{(N+1)}(c_t),\\
&\tfrac{t^{N+1}}{(N+1)!}\mathcal{I}^{(N+1)}(c_t),\\
&\tfrac{t^{N+1}}{(N+1)!}\mathcal{R}^{(N+1)}(c_t),\\
&\tfrac{t^{N+1}}{(N+1)!}\mathcal{D}^{(N+1)}(c_t),
\end{aligned} \tag{4.3}$$

for $0 \le t \le b$ and from here it becomes

$$\begin{aligned}
\|\mathcal{S}(t)-\mathcal{S}_N^M(t)\|_\infty &\le \tfrac{b^{N+1}}{(N+1)!}\|\mathcal{S}^{(N+1)}(c_t)\|_\infty,\\
\|\mathcal{I}(t)-\mathcal{I}_N^M(t)\|_\infty &\le \tfrac{b^{N+1}}{(N+1)!}\|\mathcal{I}^{(N+1)}(c_t)\|_\infty,\\
\|\mathcal{R}(t)-\mathcal{R}_N^M(t)\|_\infty &\le \tfrac{b^{N+1}}{(N+1)!}\|\mathcal{R}^{(N+1)}(c_t)\|_\infty,\\
\|\mathcal{D}(t)-\mathcal{D}_N^M(t)\|_\infty &\le \tfrac{b^{N+1}}{(N+1)!}\|\mathcal{D}^{(N+1)}(c_t)\|_\infty.
\end{aligned} \tag{4.4}$$

On the other hand, the matrix forms of PLPS are known from Lemma 2.2. Also, the expansions of Maclaurin series can be written, as $\mathcal{S}_N^M(t) = \mathbf{T}_N(t)\widetilde{\mathbf{A}}_N$, $\mathcal{I}_N^M(t) = \mathbf{T}_N(t)\widetilde{\mathbf{B}}_N$, $\mathcal{R}_N^M(t) = \mathbf{T}_N(t)\widetilde{\mathbf{C}}_N$, $\mathcal{D}_N^M(t) = \mathbf{T}_N(t)\widetilde{\mathbf{D}}_N$, respectively. Thus, for the terms $\|\mathcal{S}_N^M(t)-\mathcal{S}_N(t)\|_\infty$, $\|\mathcal{I}_N^M(t)-\mathcal{I}_N(t)\|_\infty$, $\|\mathcal{R}_N^M(t)-\mathcal{R}_N(t)\|_\infty$, $\|\mathcal{D}_N^M(t)-\mathcal{D}_N(t)\|_\infty$, we write

$$\begin{aligned}
\|\mathcal{S}_N^M(t)-\mathcal{S}_N(t)\|_\infty &= \|\mathbf{T}_N(t)(\widetilde{\mathbf{A}}_N-\mathbf{M}_N\mathbf{A}_N)\|_\infty \le \|\mathbf{T}_N(t)\|_\infty\left(\|\widetilde{\mathbf{A}}_N\|_\infty + \|\mathbf{M}_N\|_\infty\|\mathbf{A}_N\|_\infty\right)\\
\|\mathcal{I}_N^M(t)-\mathcal{I}_N(t)\|_\infty &= \|\mathbf{T}_N(t)(\widetilde{\mathbf{B}}_N-\mathbf{M}_N\mathbf{B}_N)\|_\infty \le \|\mathbf{T}_N(t)\|_\infty\left(\|\widetilde{\mathbf{B}}_N\|_\infty + \|\mathbf{M}_N\|_\infty\|\mathbf{B}_N\|_\infty\right)\\
\|\mathcal{R}_N^M(t)-\mathcal{R}_N(t)\|_\infty &= \|\mathbf{T}_N(t)(\widetilde{\mathbf{C}}_N-\mathbf{M}_N\mathbf{C}_N)\|_\infty \le \|\mathbf{T}_N(t)\|_\infty\left(\|\widetilde{\mathbf{C}}_N\|_\infty + \|\mathbf{M}_N\|_\infty\|\mathbf{C}_N\|_\infty\right)\\
\|\mathcal{D}_N^M(t)-\mathcal{D}_N(t)\|_\infty &= \|\mathbf{T}_N(t)(\widetilde{\mathbf{D}}_N-\mathbf{M}_N\mathbf{D}_N)\|_\infty \le \|\mathbf{T}_N(t)\|_\infty\left(\|\widetilde{\mathbf{D}}_N\|_\infty + \|\mathbf{M}_N\|_\infty\|\mathbf{D}_N\|_\infty\right).
\end{aligned} \tag{4.5}$$

As a next step, because of $0 \le t \le b$, $\|\mathbf{T}_N(t)\|_\infty$ is expressed as

$$\|\mathbf{T}_N(t)\|_\infty \le \max\{b^N,1\} := v_N. \tag{4.6}$$

By using the expression (4.6) into the inequality (4.5), it becomes

$$
\begin{aligned}
&\|\mathcal{S}_N^M(t) - \mathcal{S}_N(t)\|_\infty \le v_N \left(\|\widetilde{\mathbf{A}}_N\|_\infty + \|\mathbf{M}_N\|_\infty \|\mathbf{A}_N\|_\infty\right), \\
&\|\mathcal{I}_N^M(t) - \mathcal{I}_N(t)\|_\infty \le v_N \left(\|\widetilde{\mathbf{B}}_N\|_\infty + \|\mathbf{M}_N\|_\infty \|\mathbf{B}_N\|_\infty\right), \\
&\|\mathcal{R}_N^M(t) - \mathcal{R}_N(t)\|_\infty \le v_N \left(\|\widetilde{\mathbf{C}}_N\|_\infty + \|\mathbf{M}_N\|_\infty \|\mathbf{C}_N\|_\infty\right), \\
&\|\mathcal{D}_N^M(t) - \mathcal{D}_N(t)\|_\infty \le v_N \left(\|\widetilde{\mathbf{D}}_N\|_\infty + \|\mathbf{M}_N\|_\infty \|\mathbf{D}_N\|_\infty\right).
\end{aligned}
\tag{4.7}
$$

Accordingly, if the inequalities (4.4) and (4.7) are substituted in (4.2), then we gain (4.1), which completes the proof. □

Theorem 4.2 *(Error Estimation) The error problem for the SIRD model (1.1) is constructed as*

$$
\begin{cases}
e'_{1,N}(t) + \frac{\beta}{\mathcal{P}}\left(e_{1,N}(t)e_{2,N}(t) + \mathcal{I}_N(t)e_{1,N}(t) + \mathcal{S}_N(t)e_{2,N}(t)\right) = -Re_{1,N}(t) \\
e'_{2,N}(t) - \frac{\beta}{\mathcal{P}}\left(e_{1,N}(t)e_{2,N}(t) + \mathcal{I}_N(t)e_{1,N}(t) + \mathcal{S}_N(t)e_{2,N}(t)\right) + \gamma e_{2,N}(t) + \delta e_{2,N}(t) = -Re_{2,N}(t) \\
e'_{3,N}(t) - \gamma e_{2,N}(t) = -Re_{3,N}(t) \\
e'_{4,N}(t) - \delta e_{2,N}(t) = -Re_{4,N}(t) \\
e_{1,N}(0) = 0, e_{2,N}(0) = 0, e_{3,N}(0) = 0, e_{4,N}(0) = 0
\end{cases}
\tag{4.8}
$$

where

$$
\begin{aligned}
e_{1,N}(t) &= \mathcal{S}(t) - \mathcal{S}_N(t) \\
e_{2,N}(t) &= \mathcal{I}(t) - \mathcal{I}_N(t) \\
e_{3,N}(t) &= \mathcal{R}(t) - \mathcal{R}_N(t) \\
e_{4,N}(t) &= \mathcal{D}(t) - \mathcal{D}_N(t).
\end{aligned}
$$

Proof The approximate solutions (1.2) provide the SIRD model (1.1). Therefore, we get

$$
\begin{aligned}
&Re_{1,N}(t) = \mathcal{S}'_N(t) + \tfrac{\beta}{\mathcal{P}}\mathcal{S}_N(t)\mathcal{I}_N(t) \\
&Re_{2,N}(t) = \mathcal{I}'_N(t) - \tfrac{\beta}{\mathcal{P}}\mathcal{S}_N(t)\mathcal{I}_N(t) + \gamma\mathcal{I}_N(t) + \delta\mathcal{I}_N(t) \\
&Re_{3,N}(t) = \mathcal{R}'_N(t) - \gamma\mathcal{I}_N(t) \\
&Re_{4,N}(t) = \mathcal{D}'_N(t) - \delta\mathcal{I}_N(t) \\
&\mathcal{S}_N(0) = \mathcal{S}_0, \mathcal{I}_N(0) = \mathcal{I}_0, \mathcal{R}_N(0) = \mathcal{R}_0, \mathcal{D}_N(0) = \mathcal{D}_0.
\end{aligned}
\tag{4.9}
$$

Hence, subtracting model (4.9) from model (1.1), we have the error problem (4.8). As a result, the proof of the theorem is completed. □

Corollary 4.3 *If problem (4.8) is solved by using PLCM via MATLAB, then the estimated error functions* $e_{1,N,M}(t)$, $e_{2,N,M}(t)$, $e_{3,N,M}(t)$, $e_{4,N,M}(t)$ *are obtained for* $M > N$.

5. Simulations

In this section, PLCM and the error estimation method are applied to SIRD model (1.1). The explanations of the required data are presented in Table 1. Our method is applied to the model for two different scenarios. For Scenarios 1, April 4, 2020 was chosen as the starting point. Accordingly, the initial values are as follows: $\mathcal{S}_0 =$ 83,996,609; $\mathcal{I}_0 =$ 3013; $\mathcal{R}_0 =$ 302; $\mathcal{D}_0 =$ 76 [†]. Also, β, γ, δ and in SIRD model (1.1) are given in Table 2

[†]Republic of Türkiye, Ministry of Health, COVID-19 Information Platform, Available from: https://covid19.saglik.gov.tr/TR-66935/genel-koronavirus-tablosu.html

for Scenarios 1. These are identified for Türkiye's Covid-19 info. For Scenarios 2, October 31, 2020 was chosen as the starting point. Accordingly, $\mathcal{S}_0$, $\mathcal{I}_0$, $\mathcal{R}_0$, $\mathcal{D}_0$ are respectively, 83, 996, 206; 2213; 1506; 75 ‡. Also, β, γ, δ and in SIRD model (1.1) are given in Table 3. These parameters are taken from the source in [52]. The SIRD model obtained according to the determined parameters is solved using a program written in MATLAB for both scenarios. Moreover, the outcomes of PLCM and RKM (Runge-Kutta method) are compared for both scenarios. Note that the results of RKM are obtained using MATLAB and we employed numerical simulation using *ode15s* solver in MATLAB. All application results are presented in tables and graphs.

Table 1. Explanations of the solutions and the errors

Data	Explanation
$\mathcal{S}(t)$	The susceptible individuals at time t
$\mathcal{I}(t)$	The individuals infected with COVID-19 at time t
$\mathcal{R}(t)$	The individuals recovered from COVID-19 at time t
$\mathcal{D}(t)$	The individuals dead from COVID-19 at time t
$\mathcal{S}_N(t)$	The susceptible individuals at time t according to the method in Section (3)
$\mathcal{I}_N(t)$	The individuals infected with COVID-19 at time t according to the method in Section (3)
$\mathcal{R}_N(t)$	The individuals recovered from COVID-19 at time t according to the method in Section (3)
$\mathcal{D}_N(t)$	The individuals dead from COVID-19 at time t according to the method in Section (3)
$e_{1,N,M}(t)$	The estimated error function for the susceptible population according to the method in Section (4)
$e_{2,N,M}(t)$	The estimated error function for the infected population according to the method in Section (4)
$e_{3,N,M}(t)$	The estimated error function for the recovered population according to the method in Section (4)
$e_{4,N,M}(t)$	The estimated error function for the dead population according to the method in Section (4)

Table 2. The values of β, γ, δ in SIRD model (1.1) (Scenarios 1).

	Transmission rate	Recovery rate	Death rate
Parameters	β	γ	δ
Values	$1/14$	$786/23,934$	$501/23,934$
	[1/day] [44]	[Total recovered/total infected] [34]	[Total dead/total infected] [34]

Table 3. The values of β, γ, δ, in SIRD model (1.1) (Scenarios 2).

	Transmission rate	Recovery rate	Death rate
Parameters	β	γ	δ
Values	0.06194	0.04375	0.001911
	[52]	[52]	[52]

The SIRD epidemic model becomes for Scenarios 1

$$\begin{aligned}
\frac{d\mathcal{S}(t)}{dt} &= -(8.5034e-10)\ \mathcal{S}(t)\mathcal{I}(t) \\
\frac{d\mathcal{I}(t)}{dt} &= (8.5034e-10)\ \mathcal{S}(t)\mathcal{I}(t) - (0.0328)\ \mathcal{I}(t) - (0.0209)\ \mathcal{I}(t) \\
\frac{d\mathcal{R}(t)}{dt} &= (0.0328)\ \mathcal{I}(t) \\
\frac{d\mathcal{D}(t)}{dt} &= (0.0209)\ \mathcal{I}(t)
\end{aligned} \tag{5.1}$$

together with conditions

$$\begin{aligned}
&\mathcal{S}(0) = 83,996,609 \\
&\mathcal{I}(0) = 3013, \quad \mathcal{R}(0) = 302, \quad \mathcal{D}(0) = 76.
\end{aligned} \tag{5.2}$$

‡Republic of Türkiye, Ministry of Health, COVID-19 Information Platform, Available from: https://covid19.saglik.gov.tr/TR-66935/genel-koronavirus-tablosu.html

According to the solution forms in (1.2), for $N=5$ we get

$$\begin{aligned}
\mathcal{S}_5(t) &= \textstyle\sum_{n=0}^{5} a_n Q_n(t),\\
\mathcal{I}_5(t) &= \textstyle\sum_{n=0}^{5} b_n Q_n(t),\\
\mathcal{R}_5(t) &= \textstyle\sum_{n=0}^{5} c_n Q_n(t),\\
\mathcal{D}_5(t) &= \textstyle\sum_{n=0}^{5} d_n Q_n(t)
\end{aligned} \tag{5.3}$$

or by utilizing Lemma 2.2, instead of (5.3) it can be written

$$\begin{aligned}
\mathcal{S}_5(t) &= \mathbf{T}_5(t)\mathbf{M}_5\mathbf{A}_5\\
\mathcal{I}_5(t) &= \mathbf{T}_5(t)\mathbf{M}_5\mathbf{B}_5\\
\mathcal{R}_5(t) &= \mathbf{T}_5(t)\mathbf{M}_5\mathbf{C}_5\\
\mathcal{D}_5(t) &= \mathbf{T}_5(t)\mathbf{M}_5\mathbf{D}_5
\end{aligned} \tag{5.4}$$

where

$$\mathbf{A}_5 = \begin{bmatrix} a_0 & a_1 & a_2 & a_3 & a_4 & a_5 \end{bmatrix}^T, \quad \mathbf{B}_5 = \begin{bmatrix} b_0 & b_1 & b_2 & b_3 & b_4 & b_5 \end{bmatrix}^T, \quad \mathbf{C}_5 = \begin{bmatrix} c_0 & c_1 & c_2 & c_3 & c_4 & c_5 \end{bmatrix}^T,$$

$$\mathbf{D}_5 = \begin{bmatrix} d_0 & d_1 & d_2 & d_3 & d_4 & d_5 \end{bmatrix}^T, \quad \mathbf{T}_5(t) = \begin{bmatrix} 1 & t & t^2 & t^3 & t^4 & t^5 \end{bmatrix}, \quad \mathbf{M}_5^T = \begin{bmatrix} 2 & 0 & 0 & 0 & 0 & 0\\ 0 & 2 & 0 & 0 & 0 & 0\\ 2 & 0 & 4 & 0 & 0 & 0\\ 0 & 6 & 0 & 8 & 0 & 0\\ 2 & 0 & 16 & 0 & 16 & 0\\ 0 & 10 & 0 & 40 & 0 & 32 \end{bmatrix}.$$

By determining the collocation points, we obtain $t_0 = 0, t_1 = 12, t_2 = 24, t_3 = 36, t_4 = 48, t_5 = 60$ for the range $[0, 60]$. According to system (3.2), we can write

$$\begin{aligned}
\mathbf{W}_0\mathbf{A}_5 + \mathbf{G}_{1,0}\mathbf{B}_5 &= 0\\
\mathbf{W}_0\mathbf{B}_5 + \mathbf{G}_{2,0}\mathbf{B}_5 &= 0\\
\mathbf{W}_0\mathbf{C}_5 + \mathbf{G}_{3,0}\mathbf{B}_5 &= 0\\
\mathbf{W}_0\mathbf{D}_5 + \mathbf{G}_{4,0}\mathbf{B}_5 &= 0\\
\mathbf{W}_1\mathbf{A}_5 + \mathbf{G}_{1,1}\mathbf{B}_5 &= 0\\
\mathbf{W}_1\mathbf{B}_5 + \mathbf{G}_{2,1}\mathbf{B}_5 &= 0\\
\mathbf{W}_1\mathbf{C}_5 + \mathbf{G}_{3,1}\mathbf{B}_5 &= 0\\
\mathbf{W}_1\mathbf{D}_5 + \mathbf{G}_{4,1}\mathbf{B}_5 &= 0\\
&\vdots\\
\mathbf{W}_5\mathbf{A}_5 + \mathbf{G}_{1,5}\mathbf{B}_5 &= 0\\
\mathbf{W}_5\mathbf{B}_5 + \mathbf{G}_{2,5}\mathbf{B}_5 &= 0\\
\mathbf{W}_5\mathbf{C}_5 + \mathbf{G}_{3,5}\mathbf{B}_5 &= 0\\
\mathbf{W}_5\mathbf{D}_5 + \mathbf{G}_{4,5}\mathbf{B}_5 &= 0
\end{aligned} \tag{5.5}$$

where

$$\begin{aligned}
&\mathbf{W}_i = \mathbf{T}_5(t_i)\mathbf{F}_5\mathbf{M}_5,\\
&\mathbf{G}_{1,i} = (8.5034e-10)\ (\mathbf{T}_5(t_i)\mathbf{M}_5\mathbf{A}_5)\,\mathbf{T}_5(t_i)\mathbf{M}_5,\\
&\mathbf{G}_{2,i} = -(8.5034e-10)\ (\mathbf{T}_5(t_i)\mathbf{M}_5\mathbf{A}_5)\,\mathbf{T}_5(t_i)\mathbf{M}_5 + (0.0328)\ \mathbf{T}_5(t_i)\mathbf{M}_5 + (0.0209)\ \mathbf{T}_5(t_i)\mathbf{M}_5,\\
&\mathbf{G}_{3,i} = -(0.0328)\ \mathbf{T}_5(t_i)\mathbf{M}_5,\\
&\mathbf{G}_{4,i} = -(0.0209)\ \mathbf{T}_5(t_i)\mathbf{M}_5,
\end{aligned}$$

$$\mathbf{T}_5(0) = \begin{bmatrix} 1 & 0 & 0 & 0 & 0 & 0 \end{bmatrix},\quad \mathbf{T}_5(12) = \begin{bmatrix} 1 & 12 & 12^2 & 12^3 & 12^4 & 12^5 \end{bmatrix},\quad \mathbf{T}_5(24) = \begin{bmatrix} 1 & 24 & 24^2 & 24^3 & 24^4 & 24^5 \end{bmatrix},$$

$$\mathbf{T}_5(36) = \begin{bmatrix} 1 & 36 & 36^2 & 36^3 & 36^4 & 36^5 \end{bmatrix},\quad \mathbf{T}_5(48) = \begin{bmatrix} 1 & 48 & 48^2 & 48^3 & 48^4 & 48^5 \end{bmatrix},$$

$$\mathbf{T}_5(60) = \begin{bmatrix} 1 & 60 & 60^2 & 60^3 & 60^4 & 60^5 \end{bmatrix},\quad \mathbf{M}_5 = \begin{bmatrix} 2 & 0 & 2 & 0 & 2 & 0\\ 0 & 2 & 0 & 6 & 0 & 10\\ 0 & 0 & 4 & 0 & 16 & 0\\ 0 & 0 & 0 & 8 & 0 & 40\\ 0 & 0 & 0 & 0 & 16 & 0\\ 0 & 0 & 0 & 0 & 0 & 32 \end{bmatrix},\quad \mathbf{F}_5 = \begin{bmatrix} 0 & 1 & 0 & 0 & 0 & 0\\ 0 & 0 & 2 & 0 & 0 & 0\\ 0 & 0 & 0 & 3 & 0 & 0\\ 0 & 0 & 0 & 0 & 4 & 0\\ 0 & 0 & 0 & 0 & 0 & 5\\ 0 & 0 & 0 & 0 & 0 & 0 \end{bmatrix}.$$

By using (2.7), the matrix representations of the initial conditions (5.2) are expressed as follows:

$$\begin{aligned}
&\mathbf{U}_5\mathbf{A}_5 = 83,996,609, \quad \mathbf{U}_5 = \mathbf{T}_5(0)\mathbf{M}_5,\\
&\mathbf{U}_5\mathbf{B}_5 = 3013, \quad \mathbf{U}_5 = \mathbf{T}_5(0)\mathbf{M}_5,\\
&\mathbf{U}_5\mathbf{C}_5 = 302, \quad \mathbf{U}_5 = \mathbf{T}_5(0)\mathbf{M}_5,\\
&\mathbf{U}_5\mathbf{D}_5 = 76, \quad \mathbf{U}_5 = \mathbf{T}_5(0)\mathbf{M}_5,
\end{aligned} \tag{5.6}$$

where

$$\mathbf{T}_5(0) = \begin{bmatrix} 1 & 0 & 0 & 0 & 0 & 0 \end{bmatrix}.$$

Now, the obtained system by combining (5.5)-(5.6) is solved by using MATLAB. Thus, by calculating the coefficient matrices $\mathbf{A}_5$, $\mathbf{B}_5$, $\mathbf{C}_5$ and $\mathbf{D}_5$, these are written in the solution form (5.4). Consequently, our approximate solutions become as follows:

$$\begin{aligned}
\mathcal{S}_5(t) = {}& 83,996,609 - (2.1537e+02)\ t - (1.8846e+00)\ t^2 - (1.1813e-02)\ t^3 - (3.4679e-05)\ t^4 - (3.2610e-07)\ t^5,\\
\mathcal{I}_5(t) = {}& 3013 + (5.3229e+01)\ t + (4.6567e-01)\ t^2 + (2.9122e-03)\ t^3 + (8.6147e-06)\ t^4 + (7.9519e-08)\ t^5,\\
\mathcal{R}_5(t) = {}& 302 + (9.9026e+01)\ t + (8.6660e-01)\ t^2 + (5.4360e-03)\ t^3 + (1.5918e-05)\ t^4 + (1.5059e-07)\ t^5,\\
\mathcal{D}_5(t) = {}& 76 + (6.3120e+01)\ t + (5.5238e-01)\ t^2 + (3.4649e-03)\ t^3 + (1.0146e-05)\ t^4 + (9.5989e-08)\ t^5.
\end{aligned} \tag{5.7}$$

In Figure 2, the approximate solution functions of the SIRD model (5.1)-(5.2) are depicted when N is selected as $5, 8,$ and 10 for Scenarios 1. According to this figure, it is said that there is an increase in the infected population, the recovered population and the dead population, while there is a diminish in the susceptible population. In Figure 3, the approximate solution functions of (5.1)-(5.2) (the infected population $I_5(t)$, the recovered population $R_5(t)$ and the dead population $D_5(t)$) are shown for Scenarios 1. According to outcomes of the method for Scenarios 1, at 60 days, the highest rate is recovery. In Figure 4, our approximate solution functions for $N = 5$ are compared with the approximate solution functions of RKM for Scenarios 1. From here, it is concluded that the results are similar according to the two techniques. From this, it is said that our method is successful.

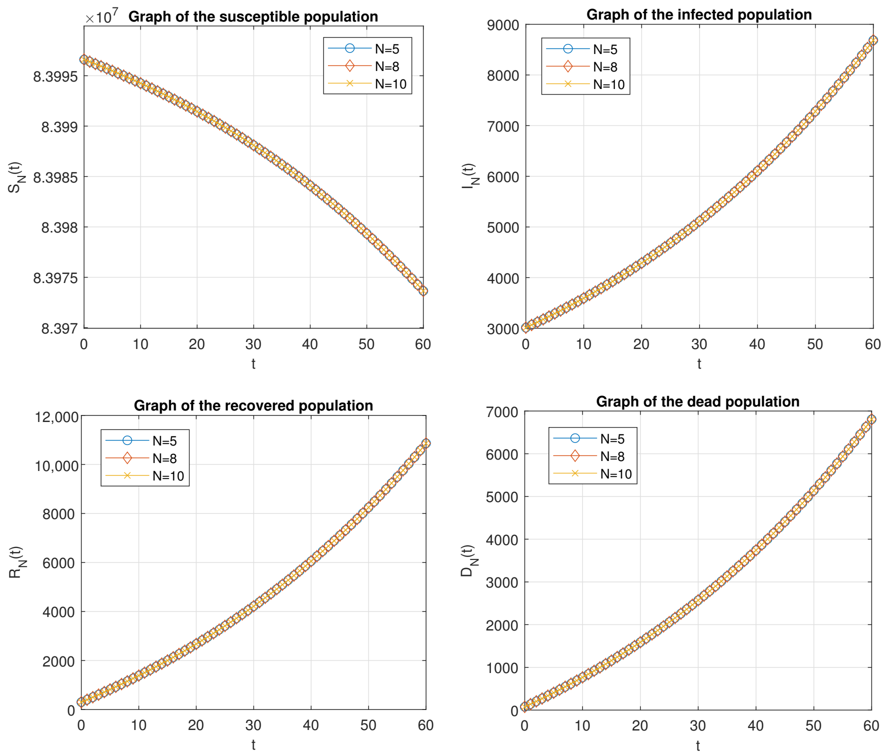

Figure 2. Plots of Pell-Lucas polynomial solutions of (5.1)-(5.2) for $N = 5$, $N = 8$, $N = 10$ (Scenarios 1).

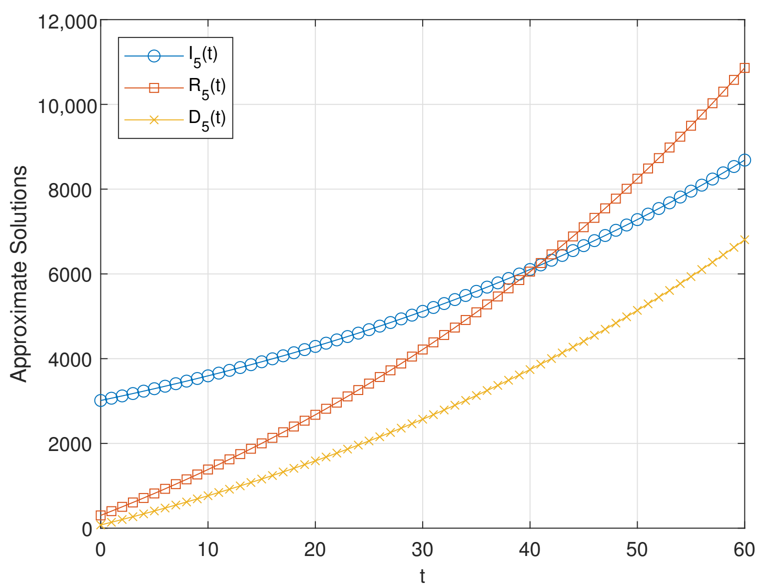

Figure 3. Comparison of the infected class, the recovered class and the dead class for $N = 5$ (Scenarios 1).

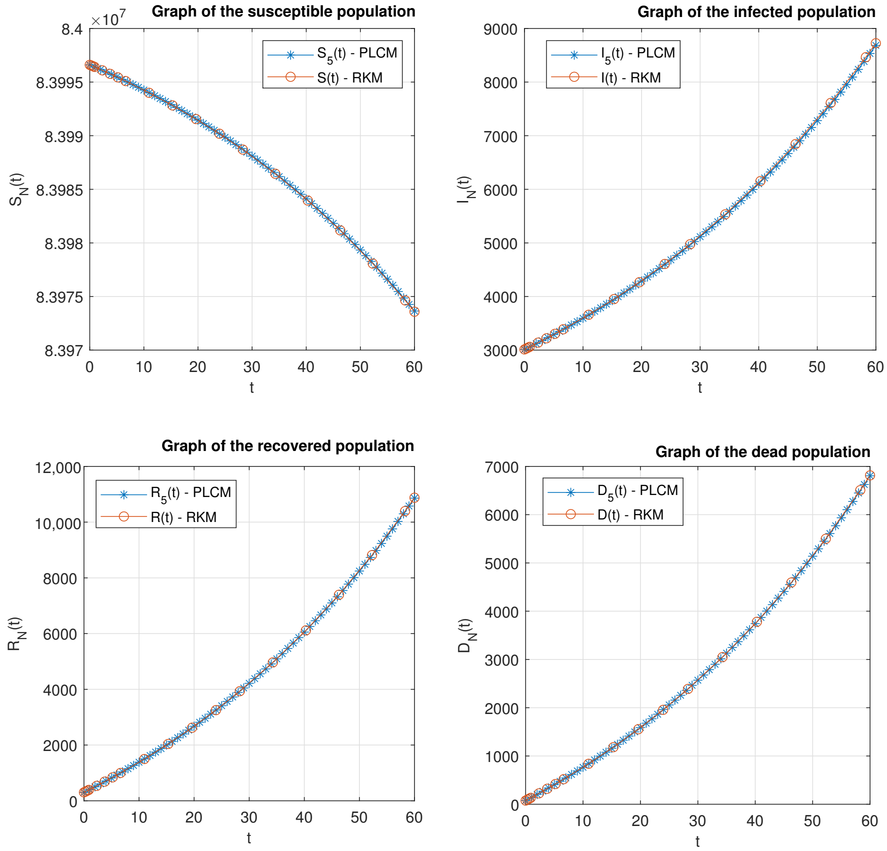

Figure 4. Plots of the comparison of Pell-Lucas polynomial solutions of (5.1)-(5.2) for $N = 5$ with RKM (Scenarios 1).

The residual error functions of (5.1)-(5.2) are compared when N is selected as $5, 8$, and 10 in Figure 5, while the estimated error functions of (5.1)-(5.2) are compared when (N, M) is selected as $(5, 6), (8, 9)$, and $(10, 11)$ in Figure 6 (Scenarios 1). Additionally, the values of these error functions at some points are given in Table 4. Moreover, the CPU times (in seconds) are demonstrated in Table 4 (Scenarios 1).

Now, let us examine the results when we apply the Pell-Lucas collocation method to the SIRD model at the range $[0, 300]$ for Scenario 2. In Figure 7, the approximate solution functions of the SIRD model are shown for $N = 8$, $N = 10$ and $N = 12$ in the range $[0, 300]$ (Scenarios 2). Accordingly, there is an increase in the infected population, the recovered population and the dead population population. As for the susceptible population, there is a diminish. In Figure 8, the approximate solution functions of the SIRD model (the infected population $I_8(t)$, the recovered population $R_8(t)$ and the dead population $D_8(t)$) are visualized for Scenario 2. Accordingly, the recovery rate is higher than the infected rate and the death rate at 300 days. In addition to these, our approximate solution functions for $N = 8$ are compared with the approximate solution functions of RKM for Scenario 2 in Figure 9. From here, it is deduced that the results of these two methods are similar and our method is successful.

Table 4. The residual absolute errors (RAE) and the estimated absolute errors (EAE) at some t points (Scenarios 1).

	RAE for $S_N(t)$		EAE for $S_N(t)$	
t_i	$N=8$	$N=10$	$(N,M)=(8,9)$	$(N,M)=(10,11)$
0	2.5056e-05	1.7783e-08	4.0250e-23	2.1607e-25
10	3.9553e-07	1.0352e-10	6.2166e-05	5.4102e-08
20	5.4813e-08	1.0179e-11	7.0338e-05	8.0230e-08
30	9.1259e-14	9.8672e-14	8.0867e-05	1.1138e-07
40	2.7207e-08	5.3320e-12	9.3632e-05	1.4853e-07
50	7.7956e-08	2.2799e-11	1.0886e-04	1.9283e-07
60	1.5689e-14	2.0004e-13	1.2527e-04	2.4498e-07
CPU time(s)	0.1563	0.3281	0.1875	0.3438
	RAE for $I_N(t)$		EAE for $I_N(t)$	
	$N=8$	$N=10$	$(N,M)=(8,9)$	$(N,M)=(10,11)$
0	4.5785e-06	1.5829e-08	1.5302e-23	8.4721e-26
10	7.1281e-08	9.2290e-11	1.1546e-05	3.3436e-08
20	9.7305e-09	9.1821e-12	1.3613e-05	3.9903e-08
30	1.4936e-13	1.5413e-13	1.6220e-05	4.7592e-08
40	4.6660e-09	4.8482e-12	1.9364e-05	5.6765e-08
50	1.3107e-08	2.0559e-11	2.3111e-05	6.7690e-08
60	5.1165e-14	6.0192e-14	2.7281e-05	8.0100e-08
CPU time(s)	0.1563	0.3281	0.1875	0.3438
	RAE for $R_N(t)$		EAE for $R_N(t)$	
	$N=8$	$N=10$	$(N,M)=(8,9)$	$(N,M)=(10,11)$
0	1.2506e-05	1.1849e-09	1.9375e-23	7.7570e-27
10	1.9802e-07	6.7026e-12	3.0915e-05	1.2607e-08
20	2.7533e-08	6.3793e-13	3.4643e-05	2.4614e-08
30	8.6016e-15	1.9237e-14	3.9482e-05	3.8939e-08
40	1.3766e-08	3.4413e-13	4.5357e-05	5.6028e-08
50	3.9605e-08	1.3239e-12	5.2367e-05	7.6410e-08
60	1.9096e-14	1.3046e-14	5.9845e-05	1.0068e-07
CPU time(s)	0.1563	0.3281	0.1875	0.3438
	RAE for $D_N(t)$		EAE for $D_N(t)$	
	$N=8$	$N=10$	$(N,M)=(8,9)$	$(N,M)=(10,11)$
0	7.9714e-06	7.4792e-10	7.1132e-23	5.8679e-28
10	1.2622e-07	4.2326e-12	1.9705e-05	8.0227e-09
20	1.7549e-08	4.1177e-13	2.2082e-05	1.5676e-08
30	9.4655e-15	4.6421e-15	2.5166e-05	2.4807e-08
40	8.7748e-09	2.0375e-13	2.8911e-05	3.5699e-08
50	2.5244e-08	8.8040e-13	3.3379e-05	4.8691e-08
60	2.7559e-15	2.3016e-14	3.8146e-05	6.4160e-08
CPU time(s)	0.1563	0.3281	0.1875	0.3438

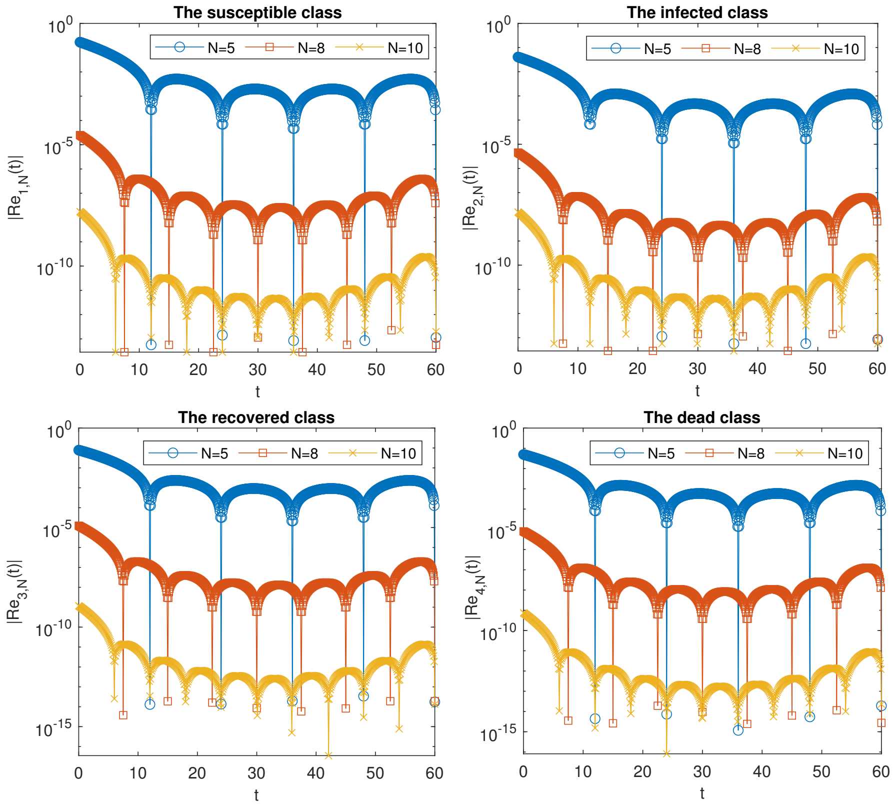

Figure 5. Comparison of the residual absolute error functions of (5.1)-(5.2) (Scenarios 1).

In Figure 10, the residual error functions of the SIRD model are compared for $N = 8$, $N = 10$ and $N = 12$. In Figure 11, the estimated error functions of the SIRD model are compared for $(N, M) = (8, 9)$, $(N, M) = (10, 11)$ and $(N, M) = (12, 13)$ for Scenarios 2. Additionally, the values of these error functions at some points are given in Table 5. Moreover, the comparisons of the results of the norms $||L||_\infty$ for Scenarios 2 are shown in Table 6. For this, the upper bound of the errors obtained with the error estimation method in Theorem 4.2 is calculated with $||L||_\infty$ by using

$$||L||_\infty = ||e_{i,N,M}||_\infty = \max\{|e_{i,N,M}|\}, \quad i = 1, 2, 3, 4.$$

According to Figures 5, 6, 10, 11 and Tables 4, 5, it is said that less errors are made when larger values of N and (N, M) are chosen for both scenarios. In addition, the results for residuals absolute errors are more accurate than the estimated ones. Thanks to the code written in MATLAB, the outcomes are quickly achieved in a very short time. This can be seen in the Table 4. Since the biggest increase is in the recovery rate, if the infected population is quarantined, the spread of the pandemic will decrease. Thus, the rate of recovery will increase further as the rate of spread will decrease. This is a positive result for the course of the pandemic. Because, if adequate isolation measures are taken, the epidemic is expected to decrease. According to all outcomes, it is observed that our techniques is successful.

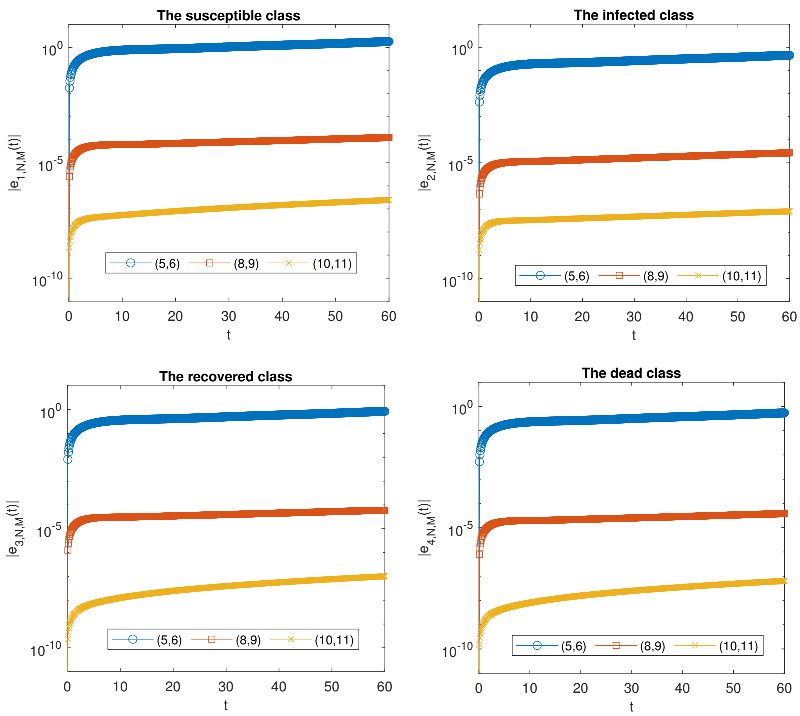

Figure 6. Comparison of the estimated absolute error functions of (5.1)-(5.2) (Scenarios 1).

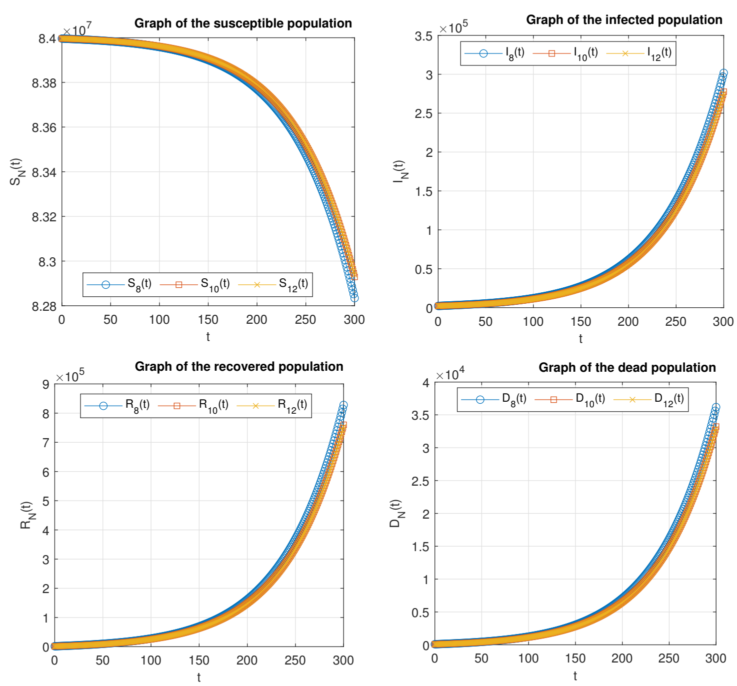

Figure 7. Plots of Pell-Lucas polynomial solutions of the SIRD model for $N = 8,\ N = 10,\ N = 12$ (Scenarios 2).

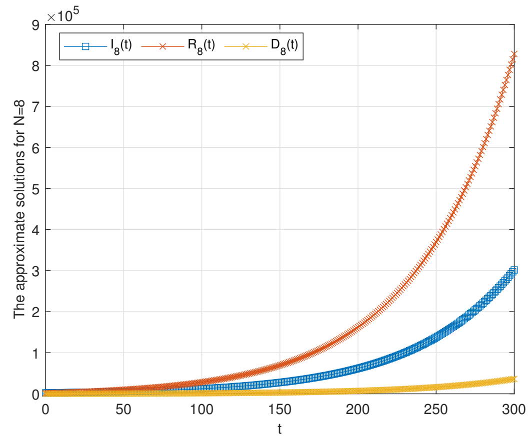

Figure 8. Comparison of the infected class, the recovered class and the dead class for $N = 8$ (Scenarios 2).

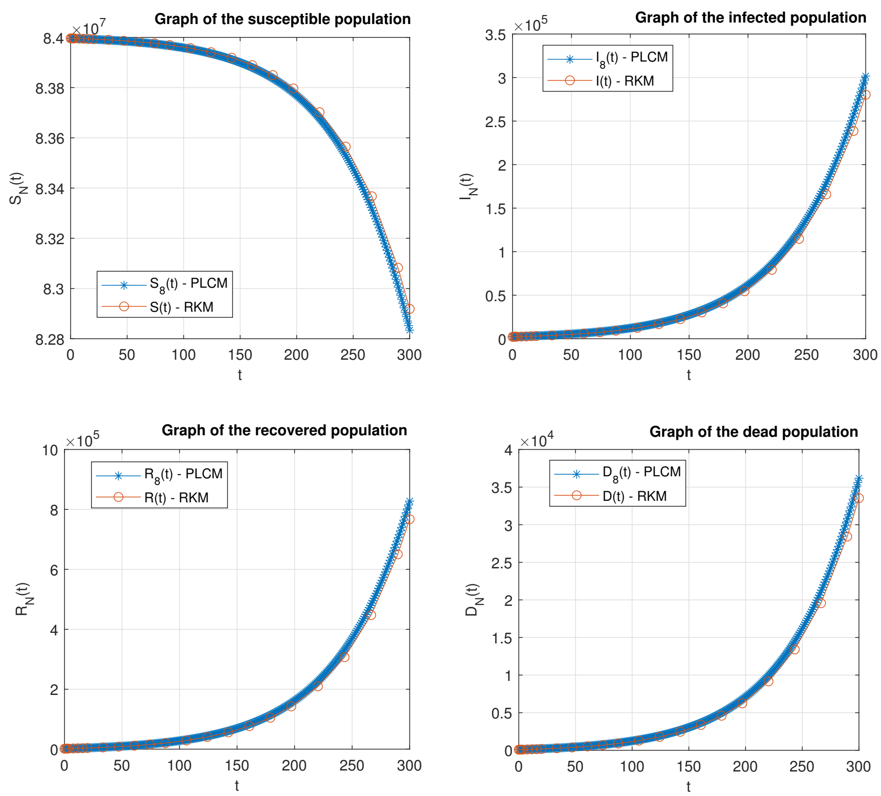

Figure 9. Plots of the comparison of Pell-Lucas polynomial solutions of the SIRD model for $N = 8$ with RKM (Scenarios 2).

Table 5. The residual absolute errors (RAE) and the estimated absolute errors (EAE) at some t points (Scenarios 2).

The Residual Absolute Errors $\|Re_{i,N}(t)\|$								
t_i	$\|Re_{1,8}(t)\|$	$\|Re_{1,12}(t)\|$	$\|Re_{2,8}(t)\|$	$\|Re_{2,12}(t)\|$	$\|Re_{3,8}(t)\|$	$\|Re_{3,12}(t)\|$	$\|Re_{4,8}(t)\|$	$\|Re_{4,12}(t)\|$
0	6.5988e-07	4.1134e-09	2.7636e-07	9.9962e-10	3.6747e-07	2.9834e-09	1.6051e-08	1.3032e-10
50	1.0693e-08	1.7949e-15	4.6200e-09	1.7949e-15	5.8186e-09	1.3003e-20	2.5416e-10	2.7244e-22
100	1.5606e-09	1.3432e-14	7.1628e-10	1.3432e-14	8.0900e-10	5.4058e-21	3.5337e-11	2.7740e-22
150	1.7563e-10	6.9599e-14	1.7563e-10	6.9599e-14	1.3609e-21	1.3221e-20	1.1181e-21	1.2983e-22
200	9.2437e-11	2.7334e-13	5.1461e-10	2.7334e-13	4.0450e-10	4.2674e-20	1.7669e-11	3.2665e-22
250	7.0006e-09	5.2242e-13	5.7860e-09	5.2242e-13	1.1637e-09	8.6970e-20	5.0831e-11	2.1521e-21
300	2.0803e-08	5.3210e-13	2.0803e-08	5.3210e-13	5.5126e-20	1.8637e-19	5.8376e-22	1.2840e-20
The Estimated Absolute Errors $\|e_{i,N,M}(t)\|$								
t_i	$\|e_{1,8,9}(t)\|$	$\|e_{1,12,13}(t)\|$	$\|e_{2,8,9}(t)\|$	$\|e_{2,12,13}(t)\|$	$\|e_{3,8,9}(t)\|$	$\|e_{3,12,13}(t)\|$	$\|e_{4,8,9}(t)\|$	$\|e_{4,12,13}(t)\|$
0	1.1553e-21	1.0507e-35	4.9937e-23	8.1328e-36	6.3181e-22	1.3172e-35	2.7598e-23	5.7535e-37
50	2.8245e-10	2.4091e-16	4.6889e-13	2.4440e-16	1.5341e-10	3.3307e-16	6.7012e-12	1.4548e-17
100	6.5971e-09	7.2594e-14	8.0097e-10	1.3664e-13	3.5174e-09	1.3427e-13	1.5364e-10	5.8649e-15
150	6.5715e-09	6.8712e-13	1.1866e-08	3.7895e-12	2.5742e-09	1.4734e-12	1.1244e-10	6.4358e-14
200	1.2618e-07	3.6054e-11	6.9077e-08	2.7527e-11	7.4385e-08	1.5031e-11	3.2491e-09	6.5657e-13
250	7.3952e-07	2.4310e-10	3.0284e-07	9.2390e-11	4.2730e-07	1.5052e-10	1.8664e-08	6.5745e-12
300	3.3360e-06	6.4680e-10	1.3500e-06	2.1807e-10	1.9249e-06	4.1954e-10	8.4078e-08	1.8326e-11

Table 6. Comparison of norms $||L||_\infty$ for Scenarios 2.

(N,M)	$\|\|e_{1,N,M}\|\|_\infty$	$\|\|e_{2,N,M}\|\|_\infty$	$\|\|e_{3,N,M}\|\|_\infty$	$\|\|e_{4,N,M}\|\|_\infty$
(8,9)	5.7766e-22	2.4968e-23	3.1590e-22	1.3799e-23
(12,13)	5.2533e-36	4.0664e-36	6.5859e-36	2.8767e-37

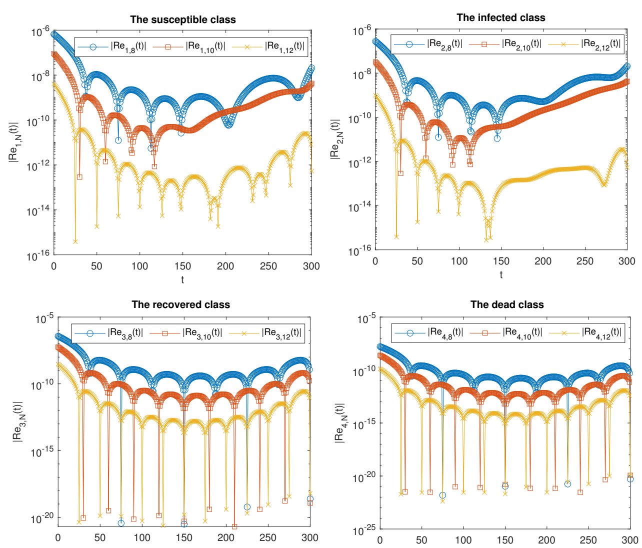

Figure 10. Comparison of the residual absolute error functions of the SIRD model (Scenarios 2).

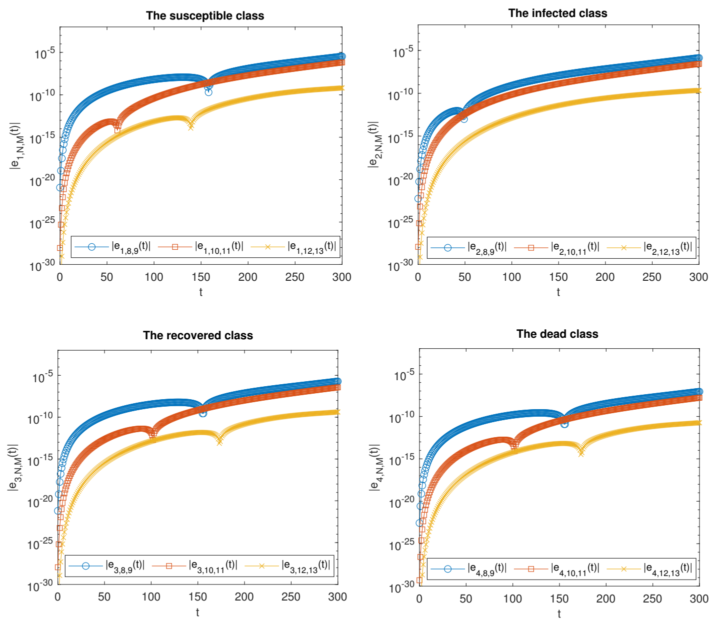

Figure 11. Comparison of the estimated absolute error functions of the SIRD model (Scenarios 2).

6. Conclusions

In this research, an SIRD model is developed to explore the current status of COVID-19 and for estimating its future evolutions in Türkiye. PLCM is implemented to this model. This method transforms the SIRD model to a matrix system that is a system of nonlinear algebraic equations. This system is solved via MATLAB, thus the approximate solutions are obtained. Moreover, the error analysis is performed in Section 4. The significance of this technique is to have information about the made error. The method is applied to the SIRD model for two different scenarios. In these two scenarios, different parameters and initial conditions are analyzed. In addition, the method is applied for the range of $[0, 60]$ in the first scenario and for the range of $[0, 300]$ in the second scenario. As a result of the application, the assumed solution functions represented the susceptible, infected, recovered and dead populations are shown in Figures 2, 3, 7, 8. According to this, the susceptible population is diminishing, while other populations is increasing. In Figure 3, while the infected population increased from 3013 to 8685, the recovered population and the died population increased, respectively, from 302 to 10,861 and from 76 to 6806 for $N = 5$ for Scenario 1. In Figure 8, while the infected population increased from 2184 to 301,712, the recovered population and the died population increased, respectively, from 1512 to 827,964 and from 84 to 36,183 for $N = 8$ for Scenario 2. Therefore, the recovered population is increased at a greater rate for both scenarios. Since the initial point, the total number of infected patients has increased for both scenarios. However, the number of the recovered patients is increasing at a greater rate. In addition, a comparison is made with RKM in Figures 4 and 9 for Scenario 1 and Scenario 2, respectively. From here, it is anticipated that the results of our techniques and the results of RKM are analogous.

On the other hand, the absolute errors (the residual and the estimated) of these solution functions for two scenarios are examined in Figures 5, 6, 10, 11 and Tables 4, 5. Accordingly, it is concluded that the error declines while the value of N rises. When these errors are compared, it is seen the that residual absolute errors give more accurate results.

When Tables 4 and 5 are analyzed for $N = 8$, it is observed that both the residual absolute errors and the estimated absolute errors of Scenario 2 (Table 5) give better results. In other words, the errors obtained by applying the method to the SIRD model are more reasonable than in Scenario 2 (Table 5). An advantage of our method is that the results can be quickly obtained by using the code created in MATLAB. Other advantage of our method is that effective outcomes are obtained from our method even if the selected N value is very small. Another advantage of our method is that the structure of the collocation method is simple and the computational cost is low. It also provides a very easy and simple procedure for solving various problems involving differential equations that model real-world phenomena. Our method has two more advantages of great importance: The first is that it can be implemented to any country by identifying the parameters in SIRD model for several countries. The results are achieved in seconds, through code created in MATLAB. In this way, precautionary measures can be taken to reduce infections. The second is that the method can be implemented for like these infections. Although, the method also has some disadvantages. First, the errors can be made when entering data into the MATLAB program. This is a problem because it does not reflect reality. Secondly, if the values of N and M chosen in the method are too large, inappropriate results may be obtained due to the increased complexity of the operations in MATLAB. Nevertheless, there was no problem in our applications as appropriate N and M values are chosen. According to all these results, it is observed that our method is the efficient method for solving the SIRD model.

References

[1] Abramson G, Kenkre VM. Spatiotemporal patterns in the Hantavirus infection. Physical Review E 2002; 66 (1): 011912. https://doi.org/10.1103/PhysRevE.66.011912

[2] Abramson G, Kenkre VM, Yates TL, Parmenter RR. Traveling waves of infection in the hantavirus epidemics. Bulletin of Mathematical Biology 2003; 65 (3): 519-534. https://doi.org/10.1016/S0092-8240(03)00013-2

[3] Adel M, Khader MM, Assiri TA, Kallel W. Numerical simulation for COVID-19 model using a multidomain spectral relaxation technique. Symmetry 2023; 15(4): 931. https://doi.org/10.3390/sym15040931

[4] Ahmed A, Salam B, Mohammad M, Akgul A, Khoshnaw SH. Analysis coronavirus disease (COVID-19) model using numerical approaches and logistic model. AIMS Bioengineering 2020; 7 (3): 130-146. https://doi.org/10.3934/bioeng.2020013

[5] Akinboro FS, Alao S, Akinpelu FO. Numerical solution of SIR model using differential transformation method and variational iteration method. General Mathematics Notes 2014; 22 (2): 82-92.

[6] Alhejili W, Khader MM, Lotfy K, El-Bary AA, Adel M. Studying of the Covid-19 model by using the finite element method: theoretical and numerical simulation. Soft Computing 2024; 28(6): 5263-5273. https://doi.org/10.1007/s00500-023-09310-6

[7] Aslan IH, Demir M, Wise MM, Lenhart S. Modeling COVID-19: Forecasting and analyzing the dynamics of the outbreak in Hubei and Turkey. Mathematical Methods in the Applied Sciences 2022; 45 (10): 6481-6494. https://doi.org/10.1002/mma.8181

[8] Atangana A, Araz Sİ. Mathematical model of COVID-19 spread in Turkey and South Africa: theory, methods, and applications. Advances in Difference Equations 2020; 2020 (1): 1-89. https://doi.org/10.1186/s13662-020-03095-w

[9] Atangana A, Araz Sİ. Modeling third waves of Covid-19 spread with piecewise differential and integral operators: Turkey, Spain and Czechia. Results in Physics 2021; 29: 104694. https://doi.org/10.1016/j.rinp.2021.104694

[10] Biazar J, Montazeri R. A computational method for solution of the prey and predator problem. Applied Mathematics and Computation 2005; 163 (2): 841-847. https://doi.org/10.1016/j.amc.2004.05.001

[11] Biazar J. Solution of the epidemic model by Adomian decomposition method. Applied Mathematics and Computation 2006; 173 (2): 1101-1106. https://doi.org/10.1016/j.amc.2005.04.036

[12] Calafiore GC, Novara C, Possieri C. A time-varying SIRD model for the COVID-19 contagion in Italy. Annual Reviews in Control 2020; 50: 361-372. https://doi.org/10.1016/j.arcontrol.2020.10.005

[13] Canto FJA, Avila-Vales EJ. Fitting parameters of SEIR and SIRD models of COVID-19 pandemic in Mexico. Preprint; 2020; 1-11.

[14] Canto FJA, Avila-Vales EJ, Garcia-Almeida GE. SIRD-based models of COVID-19 in Yucatan and Mexico. 2020. https://doi.org/10.13140/RG.2.2.10385.86889

[15] Chatterjee S, Sarkar A, Chatterjee S, Karmakar M, Paul R. Studying the progress of COVID-19 outbreak in India using SIRD model. Indian Journal of Physics 2021; 95 (9): 1941-1957. https://doi.org/10.1007/s12648-020-01766-8

[16] Djilali S, Ghanbari B. Coronavirus pandemic: A predictive analysis of the peak outbreak epidemic in South Africa, Turkey, and Brazil. Chaos, Solitons & Fractals 2020; 138: 109971. https://doi.org/10.1016/j.chaos.2020.109971

[17] Doğan N. Numerical treatment of the model for HIV infection of CD4+ T cells by using multistep Laplace Adomian decomposition method. Discrete Dynamics in Nature and Society 2012; 2012. https://doi.org/10.1155/2012/976352 2012

[18] Dönmez Demir D, Kürkçü ÖK, Sezer M. Pell–Lucas series approach for a class of Fredholm-type delay integro-differential equations with variable delays. Mathematical Sciences 2021; 15 (1): 55-64. https://doi.org/10.1007/s40096-020-00370-5

[19] Faruk O, Kar S. A Data Driven Analysis and Forecast of COVID-19 Dynamics during the Third Wave Using SIRD Model in Bangladesh. COVID 2021; 1 (2): 503-517. https://doi.org/10.3390/covid1020043

[20] Ferrari L, Gerardi G, Manzi G. Micheletti A. Nicolussi F, et al. Modeling provincial covid-19 epidemic data using an adjusted time-dependent sird model. International Journal of Environmental Research and Public Health 2021; 18 (12): 6563. https://doi.org/10.3390/ijerph18126563

[21] Fernández-Villaverde J, Jones CI. Estimating and simulating a SIRD model of COVID-19 for many countries, states, and cities. Journal of Economic Dynamics and Control 2022; 104318. https://doi.org/10.1016/j.jedc.2022.104318

[22] Gokdogan A, Yildirim A, Merdan M. Solving a fractional order model of HIV infection of CD4+ T cells. Mathematical and Computer Modelling 2011; 54 (9-10): 2132-2138. https://doi.org/10.1016/j.mcm.2011.05.022

[23] Gökdoğan A, Merdan M, Yildirim A. A multistage differential transformation method for approximate solution of Hantavirus infection model. Communications in Nonlinear Science and Numerical Simulation 2012; 17 (1): 1-8. https://doi.org/10.1016/j.cnsns.2011.05.023

[24] Harko T, Lobo FS, Mak M. Exact analytical solutions of the Susceptible-Infected-Recovered (SIR) epidemic model and of the SIR model with equal death and birth rates. Applied Mathematics and Computation 2014; 236: 184-194. https://doi.org/10.1016/j.amc.2014.03.030

[25] Hassan HN, El-Tawil MA. Series solution for continuous population models for single and interacting species by the homotopy analysis method. Communications in Numerical Analysis 2012; 2012: 1-21. https://doi.org/10.5899/2012/cna-00106

[26] Hasan S, Al-Zoubi A, Freihet A, Al-Smadi M, Momani S. Solution of fractional SIR epidemic model using residual power series method. Applied Mathematics and Information Sciences 2019; 13 (2): 153-161. http://dx.doi.org/10.18576/amis/130202

[27] Hassani H, Mehrabi S, Naraghirad E, Naghmachi M, Yüzbaşi S. An Optimization Method Based on the Generalized Polynomials for a Model of HIV Infection of $CD4^{+}$ T Cells. Iranian Journal of Science and Technology, Transactions A: Science 2020; 44 (2): 407-416. https://doi.org/10.1007/s40995-020-00833-3

[28] Horadam AF, Mahon Bro, JM. Pell and Pell-Lucas Polynomials. The Fibonacci Quarterly 1985; 23: 7-20.

[29] Horadam AF, Swita B, Filipponi P. Integration and Derivative Sequences for Pell and Pell-Lucas Polynomials. The Fibonacci Quarterly 1994; 32: 130-135.

[30] Ibrahim Y, Khader M, Megahed A, Abd El-Salam F, Adel M. An efficient numerical simulation for the fractional COVID-19 model using the GRK4M together with the fractional FDM. Fractal and fractional 2022; 6(6): 304. https://doi.org/10.3390/fractalfract6060304

[31] Ibrahim YF, Abd El-Bar SE, Khader MM, Adel M. Studying and simulating the fractional COVID-19 model using an efficient spectral collocation approach. Fractal and Fractional 2023; 7(4): 307. https://doi.org/10.3390/fractalfract7040307

[32] Jan R, Yüzbaşı Ş. Dynamical behaviour of HIV Infection with the influence of variable source term through Galerkin method. Chaos, Solitons & Fractals 2021; 152: 111429. https://doi.org/10.1016/j.chaos.2021.111429

[33] Kanth AR, Devi S. A practical numerical approach to solve a fractional Lotka–Volterra population model with non-singular and singular kernels. Chaos, Solitons & Fractals 2021; 145: 110792. https://doi.org/10.1016/j.chaos.2021.110792

[34] Karcıoğlu Ö. COVID-19: Its epidemiology and course in the world. Journal of ADEM 2020; 1 (1): 55-70.

[35] Khader MM, Adel M. Modeling and numerical simulation for covering the fractional COVID-19 model using spectral collocation-optimization algorithm. Fractal and fractional 2022; 6(7): 363. https://doi.org/10.3390/fractalfract6070363

[36] Khan SU, Ali I. Numerical analysis of stochastic SIR model by Legendre spectral collocation method. Advances in Mechanical Engineering 2019; 11 (7): 1687814019862918. https://doi.org/10.1177/16878140198629

[37] Kovalnogov VN, Simos TE, Tsitouras C. Runge–Kutta pairs suited for SIR-type epidemic models. Mathematical Methods in the Applied Sciences 2021; 44 (6): 5210-5216. https://doi.org/10.1002/mma.7104

[38] Kumar S, Kumar R, Agarwal RP, Samet B. A study of fractional Lotka-Volterra population model using Haar wavelet and Adams-Bashforth-Moulton methods. Mathematical Methods in the Applied Sciences 2020; 43 (8): 5564-5578. https://doi.org/10.1002/mma.6297

[39] Mart´nez V. A Modified SIRD Model to Study the Evolution of the COVID-19 Pandemic in Spain. Symmetry 2021; 13 (4): 723. https://doi.org/10.3390/sym13040723

[40] Mastroberardino A, Cheng Y, Abdelrazec A, Liu H. Mathematical modeling of the HIV/AIDS epidemic in Cuba. International Journal of Biomathematics 2015; 8 (04): 1550047. https://doi.org/10.1142/S1793524515500473

[41] Merdan M, Gökdoğan A, Yildirim A. On the numerical solution of the model for HIV infection of CD4+ T cells. Computers & Mathematics with Applications 2011; 62 (1): 118-123. https://doi.org/10.1016/j.camwa.2011.04.058

[42] Merdan M. Homotopy perturbation method for solving a model for HIV infection of CD4+ T cells. Istanbul Commerce University Journal of Science 2007; 6 (12): 39-52.

[43] Mohammadi H, Rezapour S, Jajarmi A. On the fractional SIRD mathematical model and control for the transmission of COVID-19: the first and the second waves of the disease in Iran and Japan. ISA transactions 2022; 124: 103-114. https://doi.org/10.1016/j.isatra.2021.04.012

[44] Ngonghala CN, Iboi E, Eikenberry S, Scotch M, MacIntyre CR, et al. Mathematical assessment of the impact of non-pharmaceutical interventions on curtailing the 2019 novel Coronavirus. Mathematical biosciences 2020; 325: 108364. https://doi.org/10.1016/j.mbs.2020.108364

[45] Niazkar M, Eryılmaz Türkkan G, Niazkar HR, Türkkan YA. Assessment of three mathematical prediction models for forecasting the COVID-19 outbreak in Iran and Turkey. Computational and Mathematical Methods in Medicine 2020; 2020. https://doi.org/10.1155/2020/7056285

[46] Ongun MY. The Laplace Adomian decomposition method for solving a model for HIV infection of CD4+ T cells. Mathematical and Computer Modelling 2011; 53 (5-6): 597-603. https://doi.org/10.1016/j.mcm.2010.09.009

[47] Osemwinyen AC, Diakhaby A. Mathematical modelling of the transmission dynamics of ebola virus. Applied and Computational Mathematics 2015; 4 (4): 313-320. https://doi.org/10.11648/j.acm.20150404.19

[48] Özdinç M, Senel K, Ozturkcan S, Akgul A. Predicting the progress of COVID-19: the case for Turkey. Turkiye Klinikleri Journal of Medical Sciences 2020; 40 (2): 117-119. https://doi.org/10.5336/medsci.2020-75741

[49] Pacheco CC, de Lacerda CR. Function estimation and regularization in the SIRD model applied to the COVID-19 pandemics. Inverse Problems in Science and Engineering 2021; 29 (11): 1613-1628. https://doi.org/10.1080/17415977.2021.1872563

[50] Pamuk S, Pamuk N. He's homotopy perturbation method for continuous population models for single and interacting species. Computers and Mathematics with Applications 2010; 59 (2): 612-621. https://doi.org/10.1016/j.camwa.2009.10.031

[51] Pamuk S. The decomposition method for continuous population models for single and interacting species. Applied Mathematics and Computation 2005; 163 (1): 79-88. https://doi.org/10.1016/j.amc.2003.10.052

[52] Pei L, Zhang M. Long-Term Predictions of COVID-19 in Some Countries by the SIRD Model. Complexity 2021; 2021. https://doi.org/10.1155/2021/6692678

[53] Rafei M, Daniali H, Ganji DD, Pashaei H. Solution of the prey and predator problem by homotopy perturbation method. Applied Mathematics and Computation 2007; 188 (2): 1419-1425. https://doi.org/10.1016/j.amc.2006.11.007

[54] Rafei M, Daniali H, Ganji DD. Variational iteration method for solving the epidemic model and the prey and predator problem. Applied Mathematics and Computation 2007; 186 (2): 1701-1709. https://doi.org/10.1016/j.amc.2006.08.077

[55] Ramadan MA, Abd El Salam MA. Spectral collocation method for solving continuous population models for single and interacting species by means of exponential Chebyshev approximation. International Journal of Biomathematics 2018; 11 (08): 1850109. https://doi.org/10.1142/S1793524518501097

[56] Secer A, Ozdemir N, Bayram M. A Hermite polynomial approach for solving the SIR model of epidemics. Mathematics 2018; 6 (12): 305. https://doi.org/10.3390/math6120305

[57] Side S, Utami AM, Pratama MI. Numerical solution of SIR model for transmission of tuberculosis by Runge-Kutta method. Journal of Physics: Conference Series 2018; 1040: 012021. https://doi.org/10.1088/1742-6596/1040/1/012021

[58] Srivastava VK, Awasthi MK, Kumar S. Numerical approximation for HIV infection of CD4+ T cells mathematical model. Ain Shams Engineering Journal 2014; 5 (2): 625-629. https://doi.org/10.1016/j.asej.2013.12.012

[59] Şahin M, Sezer M. Pell-Lucas collocation method for solving high-order functional differential equations with hybrid delays. Celal Bayar University Journal of Science 2018; 14 (2): 141-149. https://doi.org/10.18466/cbayarfbe.307282

[60] Taghipour M, Aminikhah H. Application of Pell collocation method for solving the general form of time-fractional Burgers equations. Mathematical Sciences 2022; 1-19. https://doi.org/10.1007/s40096-021-00452-y

[61] Thirumalai S, Seshadri R, Yuzbasi S. Spectral solutions of fractional differential equations modelling combined drug therapy for HIV infection. Chaos, Solitons & Fractals 2021; 151: 111234. https://doi.org/10.1016/j.chaos.2021.111234

[62] Tulu TW, Tian B, Wu Z. Modeling the effect of quarantine and vaccination on Ebola disease. Advances in Difference Equations 2017; 2017 (1): 1-14. https://doi.org/10.1186/s13662-017-1225-z

[63] Tutsoy O, Çolak Ş, Polat A, Balikci K. A novel parametric model for the prediction and analysis of the COVID-19 casualties. Ieee Access 2020; 8: 193898-193906. https://doi.org/10.1109/ACCESS.2020.3033146

[64] Umar M, Sabir Z, Amin F, Guirao JL, Raja MAZ. Stochastic numerical technique for solving HIV infection model of CD4+ T cells. The European Physical Journal Plus 2020; 135 (5): 1-19. https://doi.org/10.1140/epjp/s13360-020-00417-5

[65] Wang P, Jia J. Stationary distribution of a stochastic SIRD epidemic model of Ebola with double saturated incidence rates and vaccination. Advances in Difference Equations 2019; 2019 (1): 1-16. https://doi.org/10.1186/s13662-019-2352-5

[66] Yan QL, Tang SY, Xiao YN. Impact of individual behaviour change on the spread of emerging infectious diseases. Statistics in medicine 2018; 37 (6): 948-969. https://doi.org/10.1002/sim.7548

[67] Yusufoğlu E, Erbaş B. He's variational iteration method applied to the solution of the prey and predator problem with variable coefficients. Physics Letters A 2008; 372 (21): 3829-3835. https://doi.org/10.1016/j.physleta.2008.02.073

[68] Yuzbasi S, Karacayir M. A Galerkin-like approach to solve continuous population models for single and interacting species. Kuwait Journal of Science 2017; 44 (2).

[69] Yüzbaşı Ş. A numerical approach to solve the model for HIV infection of CD4+ T cells. Applied Mathematical Modelling 2012; 36 (12): 5876-5890. https://doi.org/10.1016/j.apm.2011.12.021

[70] Yüzbaşı Ş. An exponential collocation method for the solutions of the HIV infection model of CD4+ T cells. International Journal of Biomathematics 2016; 9 (03): 1650036. https://doi.org/10.1142/S1793524516500364

[71] Yüzbasi Ş. Bessel collocation approach for approximate solutions of Hantavirus infection model. New Trends in Mathematical Sciences 2017; 5 (4): 89-96. http://dx.doi.org/10.20852/ntmsci.2017.218

[72] Yüzbaşı Ş. Bessel collocation approach for solving continuous population models for single and interacting species. Applied Mathematical Modelling 2012; 36 (8): 3787-3802. https://doi.org/10.1016/j.apm.2011.10.033

[73] Yüzbaşı Ş, Ismailov N. A numerical method for the solutions of the HIV infection model of CD4+ T-cells. International Journal of Biomathematics 2017; 10 (07): 1750098. https://doi.org/10.1142/S179352451750098X

[74] Yüzbaşı Ş, Karaçayır M. An exponential Galerkin method for solutions of HIV infection model of CD4+ T-cells. Computational Biology and Chemistry 2017; 67: 205-212. https://doi.org/10.1016/j.compbiolchem.2016.12.006

[75] Yüzbaşı Ş, Karaçayır M. A Galerkin-Type Method for Solving a Delayed Model on HIV Infection of $CD4^+$ T-cells. Iranian Journal of Science and Technology, Transactions A: Science 2018; 42 (3): 1087-1095. https://doi.org/10.1007/s40995-018-0529-5

[76] Yüzbaşi Ş, Sezer M. An exponential matrix method for numerical solutions of Hantavirus infection model. Applications and Applied Mathematics: An International Journal (AAM) 2013; 8 (1): 9.

[77] Yüzbaşı Ş, Yıldırım G. A collocation method to solve the parabolic-type partial integro-differential equations via Pell–Lucas polynomials. Applied Mathematics and Computation 2022; 421: 126956. https://doi.org/10.1016/j.amc.2022.126956

[78] Yüzbaşı Ş, Yildirim G. A Pell–Lucas Collocation Approach for an SIR Model on the Spread of the Novel Coronavirus (SARS CoV-2) Pandemic: The Case of Turkey. Mathematics 2023; 11 (3): 697.

[79] Yüzbaşı Ş, Yıldırım G. Pell–Lucas collocation method for numerical solutions of two population models and residual correction. Journal of Taibah University for Science 2020; 14 (1): 1262-1278. https://doi.org/10.1080/16583655.2020.1816027

[80] Yüzbaşı Ş, Yıldırım G. Pell-Lucas Collocation Method to Solve Second-Order Nonlinear Lane-Emden Type Pantograph Differential Equations. Fundamentals of Contemporary Mathematical Sciences 2022; 3 (1): 75-97. https://doi.org/10.54974/fcmathsci.1035760

[81] Yüzbaşı Ş, Yildirim G. Pell-Lucas collocation method to solve high-order linear Fredholm-Volterra integro-differential equations and residual correction. Turkish Journal of Mathematics 2020; 44 (4): 1065-1091. https://doi.org/10.3906/mat-2002-55